Soft Matter

PAPER

View Article Online
View Journal | View Issue

Cite this: *Soft Matter*, 2023, **19**, 8247

Bacterial susceptibility and resistance to modelin-5†

Sarah R. Dennison, *[a] Leslie HG Morton,[a] Kamal Badiani,[b] Frederick Harris[a] and David A. Phoenix [c]

Modelin-5 (M5-NH_2) killed *Pseudomonas aeruginosa* with a minimum lethal concentration (MLC) of 5.86 μM and strongly bound its cytoplasmic membrane (CM) with a K_d of 23.5 μM. The peptide adopted high levels of amphiphilic α-helical structure (75.0%) and penetrated the CM hydrophobic core (8.0 mN m^{-1}). This insertion destabilised CM structure *via* increased lipid packing and decreased fluidity ($\Delta G_{mix} < 0$), which promoted high levels of lysis (84.1%) and *P. aeruginosa* cell death. M5-NH_2 showed a very strong affinity (K_d = 3.5 μM) and very high levels of amphiphilic α-helical structure with cardiolipin membranes (96.0%,) which primarily drove the peptide's membranolytic action against *P. aeruginosa*. In contrast, M5-NH_2 killed *Staphylococcus aureus* with an MLC of 147.6 μM and weakly bound its CM with a K_d of 117.6 μM, The peptide adopted low levels of amphiphilic α-helical structure (35.0%) and only penetrated the upper regions of the CM (3.3 mN m^{-1}). This insertion stabilised CM structure *via* decreased lipid packing and increased fluidity ($\Delta G_{mix} > 0$) and promoted only low levels of lysis (24.3%). The insertion and lysis of the *S. aureus* CM by M5-NH_2 showed a strong negative correlation with its lysyl phosphatidylglycerol (Lys-PG) content ($R^2 > 0.98$). In combination, these data suggested that Lys-PG mediated mechanisms inhibited the membranolytic action of M5-NH_2 against *S. aureus*, thereby rendering the organism resistant to the peptide. These results are discussed in relation to structure/function relationships of M5-NH_2 and CM lipids that underpin bacterial susceptibility and resistance to the peptide.

Received 31st July 2023,
Accepted 16th October 2023

DOI: 10.1039/d3sm01007d

rsc.li/soft-matter-journal

Introduction

It has been predicted that infections due to pathogenic bacteria could be instrumental in up to ten million deaths a year by 2050,[1,2] with the very real possibility that many infections may become untreatable.[3,4] A primary focus in combatting these infections has been the 'ESKAPE' pathogens, which include multi-drug resistant (MDR) forms of *Enterococcus faecium*, *Staphylococcus aureus*, *Klebsiella pneumoniae*, *Acinetobacter baumannii*, *Pseudomonas aeruginosa*, and Enterobacter species.[5,6] This group of bacteria are the major cause of life-threatening, nosocomial infections in immunocompromised and critically ill patients.[6,7] In response, antimicrobial peptides (AMPs) have been identified as promising pharmaceutical candidates for the prevention and treatment of infections caused by these pathogens.[8,9] AMPs are naturally occurring antibiotics of the innate immune system that promote bacterial cell death through multiple mechanisms, including membrane lysis and/or attack on intracellular targets.[10,11] Bacterial resistance mechanisms to the action of AMPs are known,[12,13] but the absence of specific interactors or defined mechanistic pathways minimizes the likelihood of bacteria selecting for resistance to this action.[14,15] Moreover, the non-specific nature of their antibacterial action allows AMPs to bypass the resistance mechanisms of ESKAPE and other MDR bacterial pathogens to conventional antibiotics, which generally result from selection driven by the single sites of action used by these drugs.[8,9,16,17] This property is a major driver in the development of AMPs as alternatives or adjuvants to conventional antibiotics and as potential agents to fight the clinical challenges posed by ESKAPE pathogens.[14,18] Other important properties of AMPs in this scenario are that most of these peptides act rapidly with potent, broad-spectrum antimicrobial activity but do not affect microbiota or target healthy eukaryotic cells,[8–11] although many are able to kill cancer cells.[10,19] Currently, a number of AMPs are either in clinical trials or therapeutic, topical use to treat a variety of infectious conditions,[20,21] and progress towards their systemic application for this purpose is ongoing.[22]

Despite the clear therapeutic potential of AMPs, a number of factors have impeded the full realisation of this potential and in

[a] *School of Pharmacy and Biomedical Sciences, University of Central Lancashire, Preston PR1 2HE, UK. E-mail: srdennison1@uclan.ac.uk*
[b] *Pepceuticals Limited, 4 Feldspar Close, Warrens Park, Enderby, Leicestershire, LE19 4JS, UK*
[c] *Office of the Vice Chancellor, London South Bank University, 103 Borough Road, London SE1 0AA, UK*

† Electronic supplementary information (ESI) available. See DOI: https://doi.org/10.1039/d3sm01007d

response a number of strategies to improve their efficacy have been employed,[23,24] including the production of synthetic, designed peptides.[25] A major example of these designed AMPs is the C-terminally amidated peptide, modelin-5 (M5-NH_2), which is the archetypic member of the modelin family of AMPs.[26,27] Recent studies have shown that M5-NH_2 is non-haemolytic[28] and possesses both anticancer activity[27,29,30] and the ability to kill a variety of fungi and bacteria.[26,27,30–33] The present study investigates the ability of M5-NH_2 to kill *P. aeruginosa* and *S. aureus*, which are 'ESKAPE' pathogens of critical priority on the World Health Organisation's (WHO) list of most dangerous pathogens.[34,35]

Experimental

Materials

M5-NH_2 was supplied by Pepceuticals (Leicestershire, UK), purified by HPLC to purity greater than 99% and its sequence confirmed by MALDI mass spectrometry, as KLAKKLAKLAKLAKAL-$CONH_2$. The phospholipids used were POPG: 1-palmitoyl-2-oleoyl-*sn*-glycero-3-phosphoglycerol; TOCL (1,1′,2,2′-tetraoleoyl cardiolipin): 1′,3′-bis[1,2-dioleoyl-*sn*-glycero-3-phospho]-glycerol; POPE: 1-palmitoyl-2-oleoyl-*sn*-glycero-3-phosphoethanolamine; and Lys-DOPG: 1,2-dioleoyl-*sn*-glycero-3-[phospho-rac-(3-lysyl(1-glycerol))], all of which were purchased from Avanti Polar Lipids (Alabaster, AL). M 4-(2-hydroxyethyl)-1-piperazineethanesulfonic acid (HEPES) and ethylenediaminetetraacetic acid (EDTA) was purchased from Merk Sigma-Aldrich. All buffers were prepared using ultra-pure water (resistivity 18 MΩ cm). Ringer's solution, nutrient broth and nutrient agar were purchased from Thermo Fisher Scientific (Leicestershire, UK). HPLC grade solvents were obtained from VWR International Ltd (Lutterworth, UK) and all other regents were purchased from Merk Sigma-Aldrich Company Ltd (Dorset, UK).

The preparation of bacterial cultures. Cultures of *P. aeruginosa*, strain NCIMB 8295, and *S. aureus* strain NCIMB 6571, which had been freeze-dried in 20% (v/v) glycerol and stored at −80 °C, were used to inoculate 10 ml aliquots of sterile nutrient broth. These samples were then incubated in an orbital shaker (100 rpm; 37 °C) until the exponential phase (OD = 0.6; λ = 600 nm) was reached. Each bacterial suspension was centrifuged (15 000×*g*; 10 min) to form a cell pellet using a bench top centrifuge (ALC PK 120R). The resulting cell pellet was washed three times in $\frac{1}{4}$ strength Ringer's solution and then resuspended in 1 ml of a $\frac{1}{4}$ strength Ringer's solution to ensure there was starting inoculum density of *circa* 5.8×10^8 CFU ml^{-1}.

The preparation of model membranes. Monolayers and small unilamellar vesicles (SUVs) have been shown to replicate the properties of whole cell, bacterial membranes and those with the lipid compositions shown in Table 1 were prepared to represent the cytoplasmic membranes (CM) of *P. aeruginosa* and *S. aureus*.[36,37] It has previously been shown that these lipid mixtures are reliable mimics of naturally occurring membranes of *S. aureus* and *P. aeruginosa*[38,39] and have the added advantage that they allow the quantitative analysis of interactions between bacterial membranes and AMPs.[40,41] Either these lipid mixtures, or their individual lipid components, were then separately dissolved in chloroform (1 mg ml^{-1}) and used to from monolayers, as described below. To form SUVs, these same chloroformic solutions were dried under N_2 gas and then vacuum-dried (4 hours), after which the resulting lipid films were rehydrated using 1 × PBS (pH 7.5). These rehydrated samples were then vortexed (5 min) and the resulting lipid suspensions sonicated (30 min) using a sonicator (Soniprep 150, ISTCP, USA) until clear, followed by three cycles of freeze/thawing. The resulting solutions of SUVs were then extruded eleven times through a 0.1 μm polycarbonate filter using a polar lipids mini-extruder apparatus (Avanti, UK) and diluted 10-fold using 1 × PBS (pH 7.5). Due to the labile nature of lysyl phosphatidylglycerol (Lys-PG), monolayers and SUVs that included Lys-DOPG were prepared and used immediately.[42,43]

Table 1 The lipid composition of bacterial membrane mimics. Table 1 shows the lipid compositions used to form lipid monolayers and SUVs mimetic of *S. aureus* and *P. aeruginosa* cytoplasmic membranes, which were adapted from ref. 44 and 45

	Membrane lipids			
Bacteria	TOCL (mol%)	POPG (mol%)	POPE (mol%)	Lys-PG (mol%)
P. aeruginosa	21	11	60	0
S. aureus	5	57	0	38

The antibacterial activity of M5-NH_2. To evaluate the toxicity of M5-NH_2 to bacterial cells, stock solutions of the peptide in $\frac{1}{4}$ strength Ringer's solution (1000 μM) were diluted to give concentrations in the range 3.90 μM to 1000 μM. Aliquots (1 ml) of the peptide at each concentration in this range were then separately inoculated with the *P. aeruginosa* and *S. aureus* cell suspensions prepared above (10 μl) and incubated overnight (37 °C). As a control, cultures of these bacteria were similarly treated but in the absence of M5-NH_2. After incubation, aliquots of control cultures and peptide treated cultures (10 μl) were spread onto the surface of Nutrient Agar plates and incubated overnight (37 °C; 12 h). After incubation, the plates were viewed and samples with the lowest concentration of M5-NH_2 yielding no bacterial growth was identified as the minimal lethal concentration (MLC). These experiments were repeated four times.

The membrane binding of M5-NH_2. The ability of M5-NH_2 to bind to bacterial membranes was investigated using a fluorescent probe assay. Lipid mixtures with the compositions shown in Table 1 were prepared to represent the CM of *P. aeruginosa* and *S. aureus*. Either these lipid mixtures, or their individual lipid components, were then separately dissolved in chloroform (1 mg ml^{-1}). Fluorescein-phosphatidylethanolamine (FPE; 0.5 mol%) was then added to these chloroformic solutions, which were then dried under vacuum, overnight, to create lipid films. These films were then hydrated with Tris–HCl (10.0 mM; pH 7.4) and EDTA (1.0 mM), followed by freeze-thawing five times and extrusion eleven times through an Avanti mini-extruder apparatus containing a 0.1 μm polycarbonate filter. Fluorescence was recorded using an FP-6500 spectrofluorometer (Jasco, UK), with an excitation wavelength of 492 nm, an emission wavelength of 516 nm, and excitation and emission slits set

to 5 nm. To investigate the binding of peptide to lipid vesicles, M5-NH_2 in the range 0 to 325 μM, was added to the FPE-labelled SUVs and the fluorescence monitored. The change in fluorescence (ΔF) was then determined as the fluorescence of FPE-labelled vesicles in the presence of peptide minus that of FPE-labelled vesicles in the absence of peptide. These ΔF values were then plotted against the concentration of M5-NH_2 and then fitted by non-linear least squares analysis to eqn (1):

$$\Delta F = (\Delta F_{Max}[A])/(K_d + [A]) \quad (1)$$

where [A] is the concentration of M5-NH_2, ΔF is the change in fluorescence, ΔF_{Max} is the maximum change in fluorescence and K_d, is the binding coefficient of the peptide. These experiments were repeated four times and the average K_d, derived, all as previously described.[46,47]

The conformational behaviour of M5-NH_2 in the presence of membranes. The secondary structural preferences of M5-NH_2 in the presence of various SUVs was investigated using a J-815 spectropolarimeter (Jasco, UK) at a temperature of 20 °C, which was maintained using a Peltier controller. SUVs were formed from either individual pure lipids or lipid mimics of the CM of *P. aeruginosa* and *S. aureus*, as described above. Spectral measurements were performed in 10 mm path length quartz cells (Starna Scientific, UK), which contained these SUVs mixed with stock M5-NH_2 solution (final concentration of 0.1 mg ml^{-1} in 1 × PBS (pH 7.4)) to give samples with a peptide : lipid molar ratio of 1 : 20. Both in the presence and absence of these SUVs, far-UV CD spectra were collected for M5-NH_2, where ten scans per sample were obtained using a 10 mm path-length cell. Each scan was performed over a wavelength range of 180 nm to 260 nm at 0.5 nm intervals employing a bandwidth of 1 nm and at a speed 10 nm min^{-1}. For all spectra obtained, the baseline acquired in the absence of peptide was subtracted and the percentage α-helical content of M5-NH_2 estimated using the CDSSTR method (protein reference set 3) from the DichroWeb server.[48] These experiments were repeated four times and the percentage α-helicity of M5-NH_2 was averaged.

The membrane partitioning of M5-NH_2. The insertion of M5-NH_2 into lipid monolayers was investigated at a temperature of 20 °C using a 601 M Langmuir Teflon trough (Biolin Scientific/KSV NIMA, Coventry, UK) equipped with moveable barriers. Monolayers were formed from either individual pure lipids or lipid mimics of the CM of *P. aeruginosa* and *S. aureus*, as described above. These various lipid samples mixtures were spread dropwise onto the buffer subphase (1 × PBS; pH 7.4) of the 601 M Langmuir trough using a Hamilton syringe. The solvent was allowed to evaporate for 10 min, and the monolayers were compressed by the two moveable Derlin barriers of the Langmuir trough at a velocity of 50 mm min^{-1} until a starting surface pressure of 30 mN m^{-1} had been achieved. This surface pressure corresponds to that of naturally occurring cell membranes and is generally used when constructing monolayers representative of bacterial membranes.[40,41] M5-NH_2 was injected underneath monolayers to give a final peptide concentration of 6 μM in the subphase, which was maintained at a constant surface area *via* a built-in controlled feedback system, Changes in surface pressure increases were monitored by the Wilhelmy method using a Whatman's CH1 filter paper plate and microbalance. These experiments were repeated four times and the changes in maximal surface pressure induced by M5-NH_2 averaged.

Thermodynamic analysis of M5-NH_2 and lipid monolayer interactions. Compression isotherms were generated from lipid monolayer mimics of the CM of *P. aeruginosa* and *S. aureus*, prepared as described above, and chloroformic solutions of these lipid molecules (2.5×10^{15}) were spread onto a 1 × PBS buffer subphase (pH 7.4) The solvent was allowed to evaporate for 10 min, the monolayer left to stabilize for a further 20 min and then the trough barriers were then closed at a speed of 0.22 nm^2 min^{-1} until monolayer collapse pressure was achieved. Surface pressure changes were monitored and plotted as a function of the area per lipid molecule. Corresponding experiments were then performed except that M5-NH_2 was introduced into the subphase to give a final peptide concentration of 6.0 μM. All experiments were carried out at 20 °C, repeated four times and averaged.

Thermodynamic analysis of these isotherms was undertaken and used to determine the Gibbs free energy of mixing (ΔG_{mix}) of monolayers, which provides a measure of the relative stability associated with the miscibility energetics of their pure lipid components. Thermodynamically stable and thermodynamically unstable monolayers are indicated by negative and positive values of ΔG_{mix} respectively.[40,41] ΔG_{mix} was computed according to eqn (2):

$$\Delta G_{mix} = \int [A_{1,2} - (X_1 A_1 + X_2 A_2)] d\pi \quad (2)$$

where $A_{1,2}$, is the molecular area occupied by the mixed monolayer, A_1, A_2 are the area per lipid molecule in the pure monolayers of component 1 and 2, X_1, X_2 are the molar fractions of the components and π is the surface pressure. Numerical data were calculated from the compression isotherms according to the mathematical method of Simpson.[49]

The membranolytic activity of M5-NH_2. The membranolytic ability of M5-NH_2 was investigated by observing calcein release from SUVs formed from either individual pure lipids or lipid mimics of the CM of *P. aeruginosa* and *S. aureus*, prepared as described above. These various lipid samples were dissolved in chloroform (7.5 mg ml^{-1}) and dried in a glass tube to remove the solvent, first under nitrogen and then under vacuum (*circa* 12 hours). The resulting dry lipid films were then suspended in HEPES (5.0 mM; pH 7.5) containing calcein (70 mM) and vortexed (5 min) before being sonicated (30 min) using a sonicator (Soniprep 150, ISTCP, USA). To maximise calcein encapsulation, the resulting solutions then underwent five cycles of freeze-thawing before being extruded eleven times through a 0.1 μm polycarbonate filter using a polar lipids mini-extruder apparatus (Avanti, UK). Calcein entrapped in SUVs was then separated from the free dye by elution with HEPES (5.0 mM; pH 7.5) down a Sephadex G75 column (SIGMA, UK), which had been rehydrated overnight in HEPES (20.0 mM; pH 7.5), NaCl (150 mM) and EDTA (1.0 mM).

The calcein release assay was performed by combining 25 ml of SUVs containing entrapped calcein with 50 ml of M5-NH_2 (10 mM), which was then made up to a final volume of 1 ml with HEPES (20.0 mM; pH 7.5), NaCl (150 mM) and EDTA (1.0 mM). The fluorescence intensities (FI) of calcein were monitored at 20 °C using an FP-6500 spectrofluorometer (JASCO, UK), with an excitation wavelength of 490 nm and emission wavelength of 520 nm. The fluorescence intensity induced in SUVs containing entrapped calcein by HEPES (20.0 mM; pH 7.5), NaCl (150 mM) and EDTA (1.0 mM) was taken as background leakage and that resulting from the addition of 1 μl of Triton X-100 (10%, v/v) was taken to represent 100% dye release. The percentage lysis induced by M5-NH_2 was then calculated according to eqn (3):

$$\text{Lysis (\%)} = (([FI_{M5\text{-}NH_2}] - [FI_{HEPES}])/([FI_{Triton\ X}] - [FI_{HEPES}])) \times 100 \quad (3)$$

In eqn (3), the fluorescence of calcein release by peptide is denoted by $[FI_{M5\text{-}NH_2}]$, that released by buffer as $[FI_{HEPES}]$ and that released by Triton X-100 as $[FI_{Triton\ X}]$. These experiments were repeated four times and the percentage lysis achieved by M5-NH_2 was averaged.

The effect of varying Lys-PG on the interaction of M5-NH_2 with lipid models of *S. aureus* membranes. Monolayers and SUVs mimetic of the *S. aureus* CM with the lipid compositions shown in Table 1 were prepared as described above, except that the molar ratio of TOCL to POPG was held constant at 5 : 57 mol%. and that of Lys-DOPG varied between 0 and 50 mol%. At each mol% of Lys-DOPG, monolayers were used to determine the membrane partitioning of M5-NH_2, and SUVs used to determine the membranolytic activity of the peptide, all as described above. In both cases, these experiments were repeated four times and the average levels of membrane partitioning and lysis respectively plotted as a function of Lys-PG levels.

Results

M5-NH_2 is a synthetic peptide designed to structurally mimic naturally occurring, α-helical AMPs (Fig. 1)[26,27] and in the present study, this peptide is investigated for its ability to kill *P. aeruginosa* and *S. aureus*, which are on the WHO's list of most dangerous pathogens.[34,35]

P. aeruginosa

M5-NH_2 was found to kill *P. aeruginosa* with an MLC of 5.86 μM (Fig. S1; Table 2, ESI†), indicating potent activity against the organism which was comparable to that shown by the peptide against other Gram-negative bacteria.[26,31] In general, the action of AMPs involves membrane interaction and a number of major steps in this process have been identified, including the early steps of membrane binding and conformational reassignment.[45,51] In the first of these steps, M5-NH_2 showed strong binding to SUVs mimetic of the *P. aeruginosa* CM (K_d = 23.5 μM; Table 2), which is consistent with the peptide's potent activity against the organism and indicative of a high affinity for these membranes (Table 2).[52] To characterise this binding step, the interactions of M5-NH_2 with

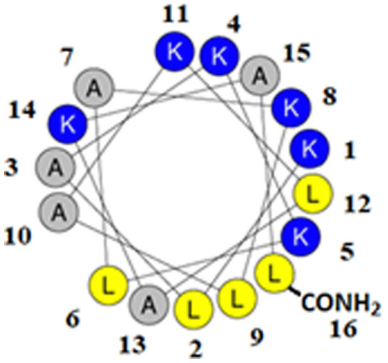

Fig. 1 Graphical analysis of M5-NH_2. Fig. 1 shows the sequence of M5-NH_2 represented as a two-dimensional axial projection using software at Heliquest, where numbers associated with individual residues represent their position in this sequence (KLAKKLAKLAKLAKAL-$CONH_2$).[50] In an α-helical conformation, the peptide shows amphiphilicity with a wide, strongly cationic polar face and a narrower apolar face. The polar face of the α-helix is primarily formed from multiple lysine residues and a C-terminal, amidated leucine residue. This residue arrangement allows electrostatic/hydrophilic interactions with anionic components of the bacterial membranes studied here, including the headgroups of CL and PG. The apolar face of the α-helix comprises alanine and leucine residues, which permits hydrophobic interactions with the apolar core regions of bacterial membranes studied here, primarily formed by the acyl chains of CL, PG and PE.

Table 2 Properties of M5-NH_2 interactions with lipid membranes. In Table 2, *P. aeruginosa* and *S. aureus* lipid mixes refer to the lipid compositions that were used to form monolayers and SUVs mimetic of the CM from these bacteria, as described in Table 1. MLCs of the peptide against *P. aeruginosa* and *S. aureus* are 5.86 μM and 147.6 μM respectively

Membrane	K_d (μM)	Lysis (%)	α-Helicity (%)	π (mN m^{-1})	ΔG_{mix}
P. aeruginosa lipid mix	23.5	84.1	75.0	8.0	>0
S. aureus lipid mix	117.6	24.3	35.0	3.3	<0
TOCL	3.5	93.1	96.0	12.3	—
POPG	6.7	74.5	86.9	9.6	—
POPE	14.9	51.0	53.0	4.9	—

SUVs formed from the individual lipid components of the CM of *P. aeruginosa* was investigated (Table 1). Anionic lipid forms around one third of the total lipid in these membranes and is predominantly formed from cardiolipin (CL) and phosphatidylglycerol (PG) (Table 1).[44] M5-NH_2 showed very high levels of binding to SUVs of TOCL (K_d = 3.5 μM; Table 2) and POPG (K_d = 6.7 μM; Table 2), which represented CL and PG respectively (Table 1). These data clearly suggested that the high affinity of M5-NH_2 for the *P. aeruginosa* CM is driven by electrostatic interactions between anionic lipid in these membranes and the peptide's cationic residues. In contrast, M5-NH_2 showed lower levels of binding with SUVs formed from POPE (K_d = 14.9 μM; Table 2), which represented the zwitterionic lipid phosphatidylethanolamine (PE); PE primarily forms the remaining two thirds of the total lipid in the CM of *P. aeruginosa* (Table 1).[44] These interactions appeared to make a minor contribution to the affinity of M5-NH_2 for the *P. aeruginosa* CM and presumably involved association of the peptide's cationic residues with

phosphate groups of PE, as shown for other AMPs.[53,54] Long range electrostatic attractive interactions similar to those involved in membrane binding are known to drive the initial targeting of bacterial membranes by AMPs, which is most probably the case for M5-NH_2 in its action against *P. aeruginosa*.[10,11]

After membrane binding, one of the most important steps in the antibacterial action of membranolytic AMPs is conformational change at the membrane interface to adopt their functional secondary structure.[45] Consistent with this step, M5-NH_2, which was unstructured in aqueous solution (Fig. 2), adopted high levels of α-helical structure in the presence of SUVs mimetic of the *P. aeruginosa* CM (α-helicity = 75.0%; Table 2 and Fig. 2). It is well established that the anisotropy of the bacterial membrane interface lowers the energy barrier for α-helix formation by AMPs[45,51] and to characterise this process for M5-NH_2, the role of individual *P. aeruginosa* CM lipids in this step was investigated (Table 1).[44,55] The peptide showed very high levels of α-helical structure in the presence of SUVs formed from TOCL (α-helicity = 96.0%) and POPG (α-helicity = 86.9%), but lower α-helicity with SUVs formed from POPE (α-helicity = 53.0%) (Table 2 and Fig. 3). These data would seem to indicate that hydrophilic interactions with CL and PG make the predominant contribution to α-helix formation by M5-NH_2 with the *P. aeruginosa* CM. It would also seem that these hydrophilic interactions are supported by a minor contribution from hydrophobic interactions between the peptide and PE in these membranes. Moreover, the involvement of both these types of interaction would appear to indicate that the α-helical structure formed by M5-NH_2 at the *P. aeruginosa* CM interface possessed amphiphilic properties (Fig. 1). It is well established that the interplay of hydrophilic and hydrophobic interactions promotes the formation of this type of secondary structure by AMPs[15,56] to facilitate their membranolytic antibacterial action.[57,58]

The next major step in the antibacterial action of AMPs is membrane insertion[45] and M5-NH_2 partitioned into monolayers mimetic of the *P. aeruginosa* CM following hyperbolic kinetics (Fig. 4). In this process, the peptide showed a rapid initial rate of insertion into these monolayers over *circa* 100 seconds, before achieving maximal surface pressures in around 1000 seconds (Fig. 4), which is consistent with the peptide's strong affinity for these membranes (Table 2). Also consistent with this strong affinity, the high levels of these maximal surface pressure changes (π = 8.0 mN m^{-1}) (Table 2 and Fig. 4) indicated deep levels of insertion and penetration into the monolayer hydrophobic region.[40,41] Following insertion, the next major step in in the antibacterial action of AMPs is membrane lysis[45] and M5-NH_2 demonstrated a strong ability to compromise the integrity of SUVs mimetic of the *P. aeruginosa* CM (lysis = 84.1%) (Table 2). In combination, these results clearly showed that the action of the peptide against *P. aeruginosa* involved membranolytic action, which receives support from thermodynamic data (Fig. 5 and 6). Monolayers mimetic of the *P. aeruginosa* CM were thermodynamically stable with values of $\Delta G_{mix} < 0$; however, in the presence of the peptide, these monolayer mimics became thermodynamically unstable with values of $\Delta G_{mix} > 0$ (Table 2). This change in ΔG_{mix} suggested that the insertion of M5-NH_2 into these monolayers had increased their lipid packing and decreased their fluidity, which is consistent with the peptide's deep insertion into the *P. aeruginosa* CM[40,41] (Table 2) as reported for other AMPs.[59–63]

To further investigate later steps in the membranolytic action of M5-NH_2 against *P. aeruginosa*, its interaction with model membranes formed from individual lipid components of the organism's CM was investigated (Table 1).[44,55] The peptide

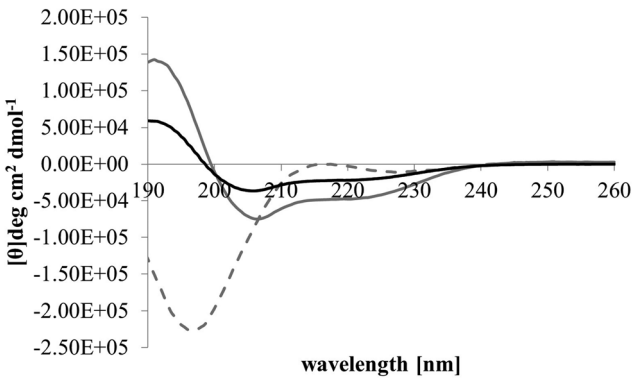

Fig. 2 Conformational analysis of M5-NH_2 in the presence of lipid mimics of the bacterial CM. Fig. 2 shows CD spectra for the conformational behaviour of M5-NH_2 in solution, and in the presence of SUVs mimetic of the bacterial CM, with the lipid compositions described Table 1. In aqueous solution (dotted grey line), the peptide displayed a maximum at 215 nm and a minimum at 195 nm, indicating that the peptide was predominantly formed from random coil and β-type structures and possessed less than 10% α-helical structure. In the presence of SUVs mimetic of the *S. aureus* CM (black line) and the *P. aeruginosa* CM (dark grey line), the peptide showed minima at 208 nm and 225 nm, and a maximum at 190 nm, which is characteristic of α-helical architecture. Analysis of these spectra showed that the peptide was 75.0% α-helical in the presence of SUVs mimetic of the *P. aeruginosa* CM, and 35.0% α-helical in the presence of those mimetic of the *S. aureus* CM (Table 2).

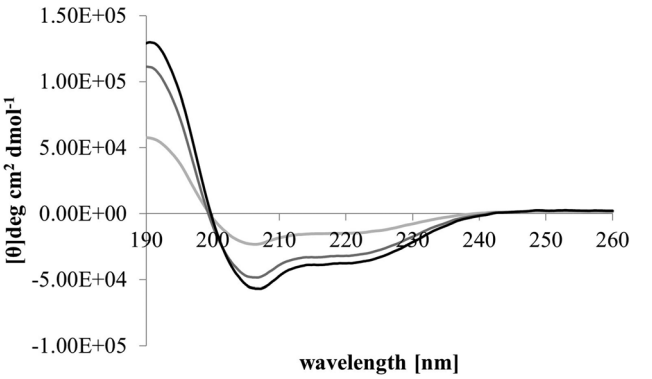

Fig. 3 Conformational analysis of M5-NH_2 in the presence of individual lipids from the bacterial CM. Fig. 3 shows CD spectra for the conformational behaviour of M5-NH_2 in the presence of SUVs formed from the individual lipid components of the *S. aureus* and *P. aeruginosa* CM (Table 1). In the case of TOCL (black line), POPG (dark grey line) and POPE (light grey line) the peptide displayed minima 208 nm and 225 nm, and a maximum at 190 nm, which is characteristic of α-helical architecture. Analysis of these spectra showed that the peptide was mainly α-helical with levels of α-helicity >85.0% in the cases of TOCL and POPG, and α-helicity = 53.0% in the case of POPE (Table 2).

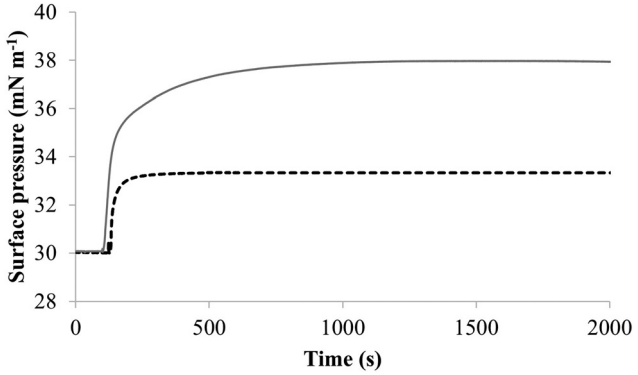

Fig. 4 The interaction of M5-NH_2 with lipid mimics of the bacterial CM. Fig. 4 shows the interaction of M5-NH_2 with monolayers mimetic of the *P. aeruginosa* and *S. aureus* CM, with the lipid compositions described Table 1. The peptide inserted into these monolayers following generally similar, hyperbolic kinetics but showed widely different rates and levels of insertion. In the case of monolayer mimics of the *S. aureus* CM (black dotted line), the peptide took *circa* 2000 seconds to achieve maximal surface pressure changes of π = 3.3 mN m^{-1} (Table 2). However, with monolayer mimics of the *P. aeruginosa* CM (dark grey line), M5-NH_2 showed much higher rates and levels of insertion, taking *circa* 1000 seconds to achieve maximal surface pressure of π = 8.0 mN m^{-1} (Table 2).

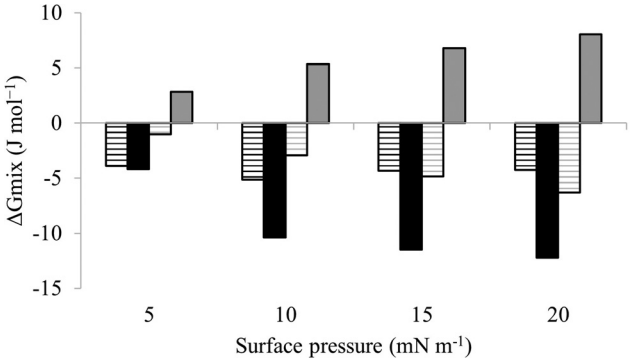

Fig. 6 Thermodynamic analysis of compression Isotherms from lipid mimics of the bacterial CM. Fig. 6 shows values of ΔG_{mix} derived from analysis of the compression isotherms depicted in Fig. 5. In the absence of M5-NH_2, ΔG_{mix} was < 0 for lipid monolayer mimics of the CM of both *S. aureus* (black striped bars) and *P. aeruginosa* (dark grey striped bars). In each case, ΔG_{mix} became progressively more negative with increasing surface pressure, indicating thermodynamic stability. In the presence of M5-NH_2 this trend was maintained for monolayer mimics of the *S. aureus* CM (black bars), except that ΔG_{mix} was enhanced for a given surface pressure. In contrast, ΔG_{mix} for monolayer mimics of the *P. aeruginosa* CM (dark grey bars) became >0 and progressively more positive with increasing surface pressure, indicating thermodynamic instability.

partitioned into monolayers formed from either TOCL or POPG following hyperbolic kinetics (Fig. 7) generally similar to those shown by M5-NH_2 with monolayers mimetic of the *P. aeruginosa* CM (Fig. 4). M5-NH_2 showed extremely rapid initial rates of insertion into these monolayers over *circa* 100 seconds, before achieving maximal surface pressures in around 500 seconds, (Fig. 7), which is consistent with the peptide's high affinity for these lipids (Table 2). Also consistent with this affinity, M5-NH_2 induced very large maximal surface pressure changes in monolayers formed from TOCL (π = 12.3 mN m^{-1}) and POPG (π = 9.6 mN m^{-1}) (Table 2 and Fig. 7). The high level of these surface pressure changes reflected the involvement of strong electrostatic interactions and an ability to deeply penetrate the hydrophobic acyl chain region of these monolayers (Table 2).[40,41] In contrast, although M5-NH_2 partitioned into monolayers formed from POPE following hyperbolic kinetics similar to those with CL and POPG, the characteristics of this process were clearly different (Fig. 7). The peptide showed much slower rates of insertion into these monolayers, achieving maximal surface pressures in around 1500 seconds, (Fig. 7), which is consistent

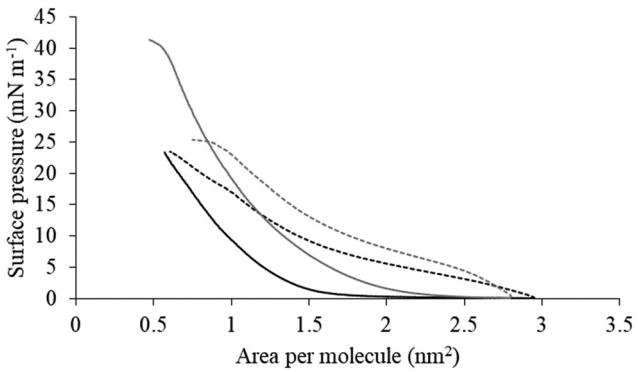

Fig. 5 Compression isotherms for lipid mimics of the bacterial CM. Fig. 5 shows compression isotherms for monolayer mimics of the *P. aeruginosa* and *S. aureus* CM, with the lipid compositions described Table 1. Shown are compression isotherms for monolayer mimics of the *S. aureus* CM (dotted black line) and that of *P. aeruginosa* (dotted dark grey line) in the absence of M5-NH2. Also shown are these isotherms for monolayer mimics of the *S. aureus* CM (black line) and that of *P. aeruginosa* (dark grey line) in the presence of the peptide. These isotherms were analysed to determine values of ΔG_{mix}, which are shown in Fig. 6.

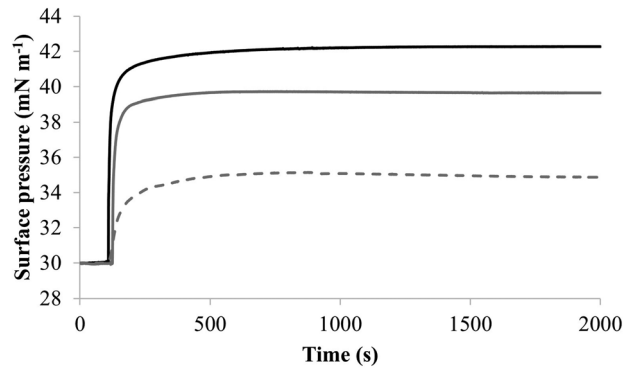

Fig. 7 The interaction of M5-NH_2 with monolayers formed from individual lipids from the bacterial CM Fig. 7 shows the interaction of M5-NH_2 with monolayers formed from the individual lipid components of the *S. aureus* and *P. aeruginosa* CM (Table 1). The peptide inserted into these monolayers following hyperbolic kinetics that were similar to those with monolayers mimetic of bacterial cytoplasmic membranes, although rates of insertion were generally faster (Fig. 5). M5-NH_2 peptide took <750 seconds to achieve maximal surface pressure changes with $\pi > 9.0$ mN m^{-1} (Table 2) for monolayers formed from TOCL (black line) and POPG (dark grey line). However, for monolayers formed from POPE (dotted light grey line), the peptide took *circa* 1500 seconds to achieve maximal surface pressure changes with π = 4.9 mN m^{-1} (Table 2).

with its weaker affinity for these lipids (Table 2). Compared to the case of TOCL and POPG, M5-NH_2 also induced lower maximal surface pressure changes in monolayers formed from POPE (π = 4.9 mN m^{-1}), indicating a weaker but significant ability to penetrate these membranes (Table 2 and Fig. 7). The peptide also showed a strong ability to lyse SUVs formed from TOCL (lysis = 93.1%) and POPG (lysis = 74.5%) but a weaker capacity to permeabilise those formed from POPE (lysis = 51.00%) (Table 2). These data clearly showed that M5-NH_2 has a strong ability penetrate and lyse model membranes formed from individual lipid components of *P. aeruginosa* membranes, which in both cases followed the rank order CL > POPG > POPE (Table 2). In combination, these data would seem to indicate that M5-NH_2 has a strong, general preference for anionic lipid in the steps of its membranolytic action against *P. aeruginosa*. These data would also appear to indicate that electrostatic interactions between the peptide's cationic residues and CL and PG drive the steps of penetration and lysis in this membranolytic action. These electrostatic interactions would appear to be complemented by a minor contribution to these steps from hydrophobic interactions between M5-NH_2 and PE (Fig. 1).

The penetration and lysis of the *P. aeruginosa* CM by M5-NH_2 involved both electrostatic and hydrophobic interaction, which clearly reflected its use of amphiphilic structure to facilitate the later steps of its membranolytic action (Fig. 1).[15] The levels of this structure formed by M5-NH_2 in the presence of single lipid SUVs followed the rank order TOCL > POPG > POPE, correlating with those of its insertion and lysis with corresponding model lipid membranes (Table 2). This correlation clearly suggested that the ability of M5-NH_2 to lyse and penetrate the *P. aeruginosa* CM was driven by the levels of its amphiphilic α-helical structure. The levels of this structure formed by the peptide with *the P. aeruginosa* CM accounted for three quarters of its architecture (Table 2), which equates to *circa* three and a half α-helical turns.[11,64] The axial length of this α-helical structure is sufficient to allow depths of insertion into the *P. aeruginosa* CM by M5-NH_2 that could penetrate the hydrophobic core of the opposing membrane leaflet.[40,41,65] These levels of insertion are clearly consistent with those shown by M5-NH_2 in its steps of penetration and lysis of the *P. aeruginosa* CM and with the associated changes to the structural properties of these membranes (Table 2). As indicated above, M5-NH_2 also showed a strong preference for anionic lipid in these later steps, as well as that of adopting amphiphilic α-helical structure at the *P. aeruginosa* CM interface. These data clearly reflected the dominance of electrostatic interactions in these steps, which suggested that amphiphilicity is the major driver of the peptides membranolytic action against *P. aeruginosa* and is supported by previous work.[31,33,66] Amphiphilic profiling has shown that M5-NH_2 exhibits high levels of amphiphilicity along the length of its α-helical conformation[33] and it has been demonstrated that this structural property drives major steps in its membranolytic action against other bacteria.[31,33,66]

In combination, these data would appear to indicate that in the early steps of its action against *P. aeruginosa*, a high affinity for anionic lipid in the CM of the organism drives binding and amphiphilic α-helix formation by M5-NH_2. In the later steps of this action, the high amphiphilicity of this α-helical structure promotes deep insertion of M5-NH_2 into the *P. aeruginosa* CM that induce high levels of lysis. These effects promote membranolytic action that leads to the death of *P. aeruginosa* and underpins the potent activity of M5-NH_2 against the organism, which is represented schematically in Fig. 8.

S. aureus

M5-NH_2 killed *S. aureus* with an MLC of 147.6 μM, representing activity over twenty-five times lower than that against *P. aeruginosa* and clearly showing *S. aureus* to be resistant to the peptide (Fig. S1 and Table 2, ESI†), which is consistent with previous work.[26,66] The capacity for potent membranolytic activity appears to generally underpin the antibacterial activity of M5-NH_2, which suggested that changes to this capacity may be involved in the resistance of *S. aureus* to the peptide's action.[26,31,33,66] Consistent with this suggestion, M5-NH_2 displayed low levels of binding to SUVs mimetic of the *S. aureus* CM (K_d = 117.6 μM) that were over five times lower than in the case of *P. aeruginosa*, reflecting the peptide's weaker activity against the former organism (Table 2). The peptide also adopted low levels of amphiphilic α-helical structure in the presence of these SUVs (Fig. 4), which accounted for around one third of its structure (35.0%) and is equivalent to *circa* one and a half α-helical turns (Table 2).[11,64] Compared to the case of *P. aeruginosa*, these levels of amphiphilic α-helical structure were two thirds lower (Table 2), which would clearly be predicted to reduce the peptide's ability to penetrate and lyse the CM of *S. aureus*.[57,58] Confirming this prediction, the insertion of M5-NH_2 into monolayer mimics of these membranes induced low maximal surface pressure changes (π = 3.3 mN m^{-1}), which were around one fifth of those with *P. aeruginosa* and indicated low levels of insertion into these monolayers (Table 2). Although showing similar kinetics, the peptide's insertion into monolayer mimics of the *S. aureus* CM was much slower than that of *P. aeruginosa*, taking two-fold longer to reach maximal surface pressures (Fig. 4). This slower kinetics of insertion reflected the much lower affinity of the peptide for these monolayers, as compared to the corresponding case with the *P. aeruginosa* CM (Table 2). Consistent with these monolayer data, M5-NH_2 also displayed a weak ability to induce the lysis of SUVs mimetic of the *S. aureus* CM (lysis = 24.5%;), which was over two thirds lower than that in the case of *P. aeruginosa* (Table 2). The levels of these model membrane associations suggested that the interactions of M5-NH_2 with the *S. aureus* CM were more associated with their head-group and upper regions than the deeper regions indicated in the case of *P. aeruginosa* (Table 2).[40,41] This suggestion was supported by thermodynamic data (Fig. 5 and Fig. 6) showing that, in contrast to *P. aeruginosa*, monolayer mimics of the *S. aureus* CM were thermodynamically unstable with values of $\Delta G_{mix} > 0$ (Table 2). However, these monolayers were rendered thermodynamically stable by the presence of M5-NH_2 with values of $\Delta G_{mix} < 0$ (Table 2) and this change in ΔG_{mix} suggested that insertion of the peptide into monolayer mimics of the *S. aureus* CM had decreased their lipid packing density and increased their membrane fluidity.[40,41] These changes in membrane properties

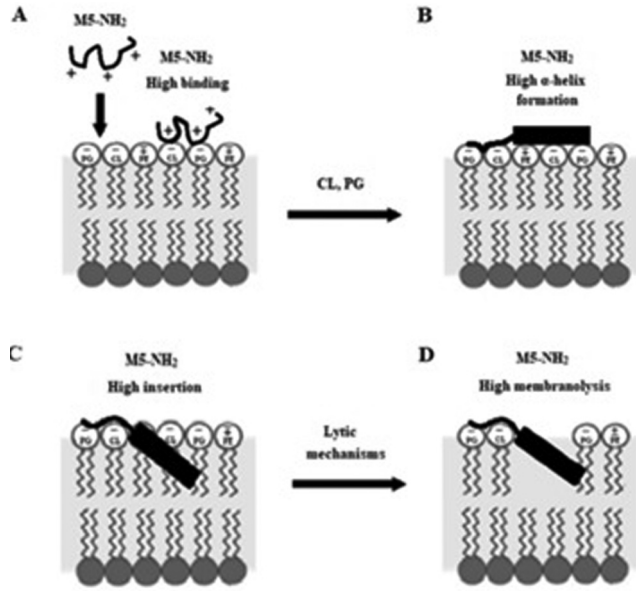

Fig. 8 A schematic representation of the membranolytic action of M5-NH_2 against *P. aeruginosa*. In the first major step of the action of M5-NH_2 against *P. aeruginosa*, electrostatic attraction facilitates targeting of the CM and promotes high levels of binding to the headgroups of PG and CL by the peptide (Fig. 8A). In the next major step, the anisotropic environment of the CM interface promotes high levels of amphiphilic α-helical structure in M5-NH_2, which potentially possesses a hydrophobicity gradient (Fig. 8B). The tilted characteristics and/or the amphiphilicity of this structure then drives the major step of insertion by the peptide into the *P. aeruginosa* CM, which leads to penetration of the hydrophobic core region of the membrane (Fig. 8C). In the final major step, the insertion of the peptide promotes a range of effects, such as increased lipid packing and decreased fluidity, that lead to destabilisation and lysis of the CM, followed by *P. aeruginosa* cell death (Fig. 8D). This membranolytic action is consistent with the use of pore forming mechanisms, such as toroidal pores, and potentially involves other effects, including anionic lipid clustering and tilted peptide destabilisation of the CM.

are consistent with the association of the peptide with the headgroup and upper regions of *S. aureus* membranes,[40,41] and similar data have previously been reported.[33,67] In combination, these data would seem to indicate that characteristics of the *S. aureus* CM had lowered the capacity M5-NH_2 to achieve the levels of conformational change and membrane interaction associated with the major steps in its action against *P. aeruginosa*. The overall effect of these weaker interactions appeared to be to lower the ability M5-NH_2 to engage in membranolytic activity against *S. aureus*, which contributed to the organism's resistance to the action of the peptide.

A primary characteristic of bacterial membranes that influences the activity of AMPs is differences in the lipid composition of these membranes and a major difference between the CM of *S. aureus* and *P. aeruginosa* is the occurrence of the cationic lipid Lys-PG (Table 1).[44,55] The lipid is absent from the CM of *P. aeruginosa*[55] but accounts for around four fifths of the lipid content in the case of the *S. aureus* CM (Table 1)[44] and is known to be an important mediator in the resistance of the organism to the action of AMPs.[38,68–73] Lys-PG was represented by Lys-DOPG and the ability of the lipid to influence the interaction of M5-NH_2 with the *S. aureus* CM was investigated by varying levels of the lipid in lipid mimics of these membranes where the CL : PG ratio (5 : 57) was held constant (Fig. 9 and Fig. S2, ESI†). Regression analysis of the data shown in Fig. 9 revealed a strong inverse correlation between the levels of Lys-DOPG in these *S. aureus* CM mimics and those of the penetration and lysis levels induced by the peptide ($R^2 > 0.98$; Fig. 9). These results were consistent with studies on the membranolytic action of other AMPs against *S. aureus* and clearly indicated that Lys-DOPG was able to attenuate the interaction of M5-NH_2 with these *S. aureus* CM mimics.[38] In the absence of Lys-DOPG, M5-NH_2 showed high levels of insertion (π = 10.0 mN m^{-1}) and lysis (lysis = 76.6%) (Fig. 9) with these membrane mimics, reflecting the peptide's strong preference for anionic lipid (Table 2).[26,31,33] Increasing the Lys-DOPG content of these membranes led to decreases in the levels of penetration and lysis shown by M5-NH_2, although they

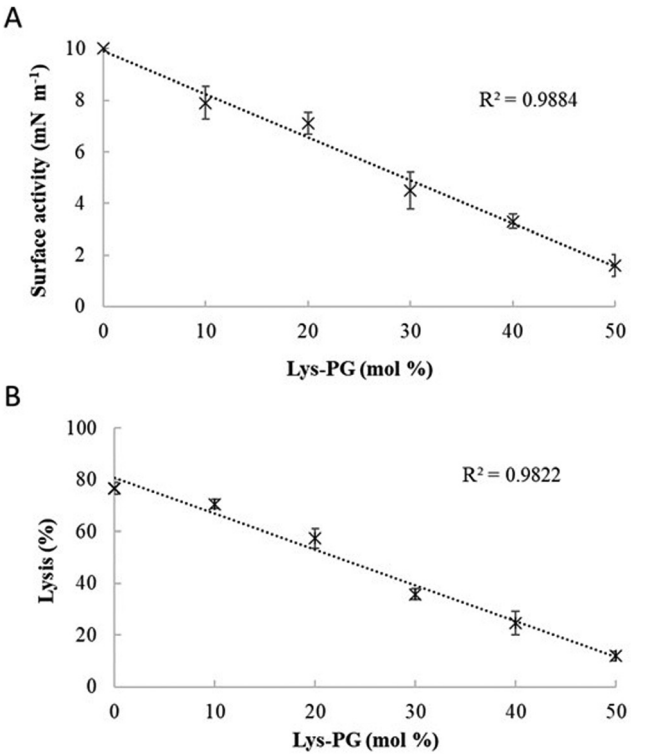

Fig. 9 The effect of varying Lys-PG on the interaction of M5-NH_2 with lipid models of *S. aureus* membranes. Fig. 9 shows the effect of varying Lys-PG content on the ability of M5-NH_2 to penetrate lipid monolayers (Fig. 9A) and induce the lysis of SUVs (Fig. 9B) mimetic of the *S. aureus* CM where the TOCL : POPG content was held constant at a physiological ratio of 5 : 57. In both cases, regression analysis showed a strong inverse correlation between the levels of Lys-PG in these membranes and those of the penetration and lysis induced by the peptide ($R^2 > 0.98$). As can also be seen from Fig. 9A and B, at physiological levels of the lipid (38 mol%), the levels of the membrane interactions induced by M5-NH_2 (π = 3.3 mN m^{-1}; lysis = 24.3%) were around one third of those in the case of membranes where Lys-PG was mot included (π = 10.0 mN m^{-1}; lysis = 76.6%). Data points shown Fig. 9A and B were derived from experimental membrane insertion and lysis curves for M5-NH_2 shown in Fig. S2 (ESI†). In both Fig. 9A and B, error bars are the standard deviation of the data about the mean value.

remained high at lower levels of the lipid (Fig. 9). At 10 mol% Lys-DOPG, the peptide inserted deeply into these lipid membrane mimics (π = 7.9 mN m^{-1}) and induced high levels of lysis (lysis = 70.5%) (Fig. 9) which is consistent with recent studies on *Bacillus subtilis*.[33] Lys-PG forms around 10 mol% of *B. subtilis* membranes[74,75] and M5-NH_2 induced similar levels of membrane penetration and lysis in its potent membranolytic action against the organism.[33] At 38 mol% POPG, which corresponds to physiological levels of Lys-PG in *S. aureus* membranes, the levels of insertion and lysis shown by the peptide were over three-fold lower relative to membranes lacking Lys-DOPG (Fig. 9). Increasing Lys-DOPG above physiological levels has been shown to lead to the eventual inability of AMPs to penetrate and lyse membranes of *S. aureus*, which presumably would be the case with M5-NH_2.[76]

In combination, these data indicate that in the early steps of its action against *S. aureus*, membrane binding and amphiphilic α-helix formation by M5-NH_2 are attenuated by some factor in the membranes of the organism, relative to the case of *P. aeruginosa*. In the later steps of this action, the reduced levels and amphiphilicity of this α-helical structure promotes insertion of M5-NH_2 into the upper reaches of *P. aeruginosa* membranes that induce low levels of lysis. These effects appear to be related to the presence of Lys-PG in the *S. aureus* CM and decrease the peptide's capacity for membranolytic action to the extent that they effectively promote the resistance of *S. aureus* to this action, which is represented schematically in Fig. 10.

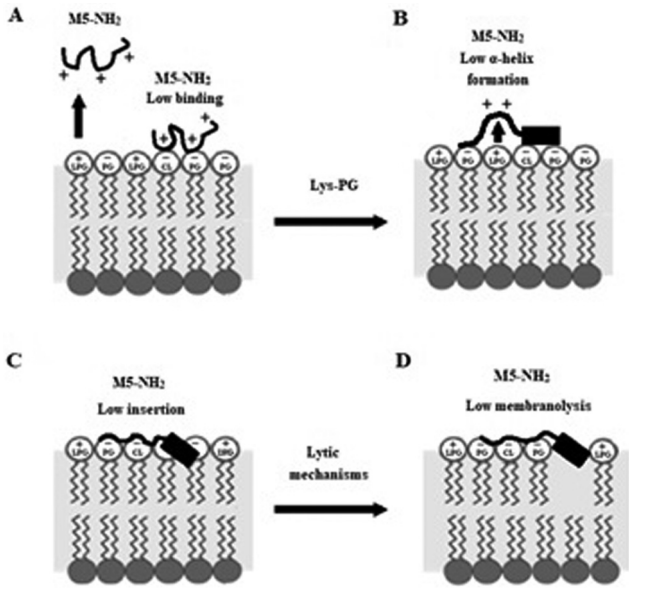

Fig. 10 A schematic representation of *S. aureus* resistance of to the membranolytic action of M5-NH_2 In the action of M5-NH_2 against *S. aureus*, Lys-PG mediated effects attenuate the interactions of the peptide with the organism's CM relative to corresponding steps in the action of the peptide against *P. aeruginosa* (Fig. 8). In the first major step, electrostatic repulsion effects due to Lys-PG reduce the ability of the peptide to target the *S. aureus* CM, resulting in lower levels of binding to the headgroups of PG and CL (Fig. 10A). In the next major step, M5-NH_2 adopts lower levels of α-helical structure due to Lys-PG mediated electrostatic repulsion effects that raise the energy barrier for this process (Fig. 10B). The resulting loss of tilted characteristics and/or amphiphilicity of this structure reduces insertion of the peptide into the *S. aureus* CM to depths that are associated with the upper regions of the membrane (Fig. 10C). In the final major step, the insertion of M5-NH_2 promotes a range of effects, such as decreased lipid packing density and increased fluidity, that stabilise the CM and reduce the levels of lysis induced by the peptide, thereby rendering *S. aureus* resistant to M5-NH_2 (Fig. 10D). The Lys-PG mediated inhibition of the peptide's membranolytic action appears to be the major mechanism used by *S. aureus* to resist M5-NH_2, but, as described in the text, there is also the possibility that other mechanisms may make minor contributions to this resistance.

Discussion

The increasing occurrence and widening antibiotic resistance of *P. aeruginosa* strains with MDR is critical[77] and methicillin-resistant *S. aureus* (MRSA) is tolerant to almost all known conventional antibiotics.[78] In both cases, this situation has been exacerbated by the emergence of resistance to the last-resort drugs used to eradicate infections due to these bacteria.[79] AMPs show a strong potential for development as agents to treat infections due to *P. aeruginosa*, and *S. aureus*[80–83] and in response, this potential was investigated for M5-NH_2, which is a peptide designed to mimic naturally occurring α-helical AMPs.[26,27]

M5-NH_2 showed potent activity against *P. aeruginosa* that was in the very low micromolar range and appeared to involve the lysis of the organism's CM (Fig. S1 and Table 2, ESI†), clearly implying that the peptide was able to traverse the barrier posed by the outer membrane (OM) of *P. aeruginosa*.[84,85] The OM of *P. aeruginosa* is essentially a bilayer formed by an external leaflet, primarily composed of anionic lipopolysaccharides (LPS), and an internal leaflet predominantly comprising phospholipids, that is spanned by specific uptake channels and non-specific porins.[86] Potentially, there are three major routes by which antimicrobial compounds can traverse the OM of *P. aeruginosa*: diffusion directly through the OM or *via* porins, or translocation through electrostatic interaction with LPS and self-promoted uptake.[85,87,88] Diffusion through porins is restricted to small hydrophilic molecules and, like most AMPs, the molecular weight of M5-NH_2 (1.7 kDa)[26] would be too high to permit use of this pathway.[89] Both remaining pathways have been demonstrated for AMPs with comparable positive charge to M5-NH_2, although self-promoted uptake appears to be the pathway most favoured by these strongly cationic peptides.[90–93]

To gain insight into the interaction of M5-NH_2 with the CM of *P. aeruginosa*, individual, major steps in these interactions were investigated and a synthesis of these data allowed a putative scheme for the action of the peptide against *P. aeruginosa* to be constructed (Fig. 8). In first of these steps, M5-NH_2 shows a strong affinity for the *P. aeruginosa* CM that is predominantly driven by high levels of binding to anionic lipids in these membranes (Table 2). This binding involves electrostatic interactions between the negative charge of phosphate moieties in CL and PG headgroups and the peptide's strong positive charge, which results from its multiple lysine residues and C-terminal amide moiety (Fig. 8A and Fig. 1).[26] However, the binding of M5-

NH_2 to CL was the highest recorded for the peptide and was around two-fold stronger than in the case of PG, reflecting differences in their head-group charge (Table 2). CL has a charge of −2 due to its two phosphate moieties whereas that of PG has a charge of −1 due to its single phosphate group.[94] Taken with the *circa* two-fold higher occurrence of CL over PG in the *P. aeruginosa* CM, this would appear to indicate that CL is the predominant mediator of M5-NH_2 binding to these membranes (Table 1). The peptide showed an affinity for PE that was over four-fold lower than that for CL, which appeared to indicate that interaction with this lipid made a minor contribution to the peptide's binding of the *P. aeruginosa* CM (Table 2). The binding of AMPs to PE generally involves electrostatic interaction between their cationic residues and the phosphate moiety in the lipid's zwitterionic headgroup, which would appear to be the case M5-NH_2.[53,54] Interestingly, recent studies have suggested that the greater accessibility of phosphate moieties in PE head-groups compared to that in phosphatidylcholine (PC) head-groups may play a role in the selective binding of AMPs to bacterial membranes.[53] PC is the major zwitterionic lipid in eukaryotic membranes[55,95] and M5-NH_2 shows negligible interaction with these membranes[28,32] but strong interaction with bacterial membranes that is comparable to that found here for the *P. aeruginosa* CM (Table 2).[31–33]

The next two steps in the interaction of M5-NH_2 with the *P. aeruginosa* CM were the closely coupled events of α-helix formation and insertion (Fig. 8B and C); the coupling of these events makes the insertion of AMPs into bacterial membranes energetically less costly.[45] The process of α-helix formation by AMPs is primarily driven by the low dielectric properties and interfacial anisotropy of the bacterial CM and reduces the cost of peptide insertion through the formation of hydrogen bonds between backbone amide and carbonyl groups of these α-helices.[96,97] M5-NH_2 adopted high levels of α-helical structure at the interface of the *P. aeruginosa* CM (Table 2 and Fig. 8B) and the strong amphiphilicity of this structure (Fig. 1) appeared to be the major driver of the peptide's insertion into these membranes (Fig. 8C), which is consistent with other studies on M5-NH_2.[30,31,33,66]

Insertion into the *P. aeruginosa* CM involves electrostatic interactions between the peptide's cationic polar face, comprising lysine residues and a C-terminal amide, and anionic lipid head-groups in these membranes (Fig. 1). It has previously been suggested that these positively charged residues may play a number of roles in promoting the insertion of M5-NH_2 into bacterial membranes.[33] These residues are evenly distributed along the α-helical long axis of the peptide (Fig. 1), which would tend to maximise their access to CL and PG headgroups in the *P. aeruginosa* CM (Fig. 8A). Indeed, this distribution may contribute to the very high affinity of M5-NH_2 for CL (Table 2), given that the anionic moieties in the head-group of this lipid are far more accessible to AMPs than those of other membrane lipids.[98]

Concomitant with the electrostatic interactions of its polar face, the apolar face of M5-NH_2, comprising alanine and leucine residues, engages in hydrophobic interactions with the apolar core of the *P. aeruginosa* CM (Fig. 1). Collectively, these interactions lead to deep penetration of this hydrophobic core region by M5-NH_2, which induces increased lipid packing, decreased membrane fluidity and the destabilization of these membranes (Table 2 and Fig. 8C). Most recently, the α-helical structure formed by M5-NH_2 was shown to possess an asymmetric distribution of hydrophobicity along the α-helical long axis.[33] This structural feature, or hydrophobicity gradient, is characteristic of tilted AMPs and drives the deep, oblique insertion of these peptides into bacterial membranes.[99] In the case of M5-NH_2, the peptide's hydrophobicity gradient promoted oblique insertion into the CM of *B. subtilis* that led to depths of insertion and a mode of membrane destabilization that showed similarities to those found here for *P. aeruginosa* (Fig. 8).[33] Given the high levels of α-helical structure adopted by the peptide, these observations suggest that M5-NH_2 nay have the potential to promote its penetration and lysis of the *P. aeruginosa* CM using tilted mechanisms. Moreover, it is interesting to note that the polar face of M5-NH_2 face is interrupted by hydrophobic residues, namely a leucine and two alanine residues, which is clearly a case of imperfect amphiphilicity (Fig. 1).[100] This form of imperfect amphiphilicity appears able to promote high antimicrobial activity and selectivity, although the mechanisms underlying this ability are often unclear.[100–103] However, in the case of M5-NH_2, the leucine and alanine residues in the α-helical polar face occur at positions 7, 12 and 15 of the peptide's sequence (Fig. 1), indicating that they are distributed along the hydrophobicity gradient possessed M5-NH_2.[33] As shown for other residues in tilted peptides, a role of these leucine and alanine residues might be to provide the balance between amphiphilicity and hydrophobicity required to promote the oblique insertion of M5-NH_2 into the CM of *P. aeruginosa* and other bacteria.[104] It has also been suggested that the lysine residues possessed by M5-NH_2 could contribute to its oblique insertion into the CM of bacteria through the snorkelling mechanism.[33] Using this mechanism, the long hydrocarbon side chains of these residues would extend into the hydrophobic core region of the *P. aeruginosa* CM, permitting deeper levels of penetration by the peptide's tilted structure, as shown for other AMPs.[66,105,106]

In a final major step of the action M5-NH_2 against *P. aeruginosa*, the insertion of the peptide into the organism's CM and the resulting destabilization leads to high levels of lysis and ultimately, cell death (Fig. 8D). It would seem that this action is unlikely to involve the formation of a membrane spanning pore by M5-NH_2, such as the barrel stave model,[10,11,14,15] due to the relatively short length of the peptide.[33] However, studies on other bacteria, have suggested that the antibacterial action of M5-NH_2 may involve mechanisms based on tilted peptide formation, the toroidal pore model and the carpet mechanism.[31,33] To gain further insight into mechanisms underpinning the action of M5-NH_2 against *P. aeruginosa*, the role of individual lipid components of the organism's membranes in the steps of α-helix formation, insertion and lysis were investigated.

M5-NH_2 showed levels of α-helicity, insertion and lysis with PE membranes that were at least a third lower than those of anionic lipid, indicating a minor, but not inconsiderable,

contribution to steps in the membranolytic action of M5-NH_2 against *P. aeruginosa* (Table 2). PE is known to play a number of roles in the antibacterial action of AMPs[107] and can specifically interact with α-helical AMPs to inhibit their antibacterial action.[108] Some α-helical AMPs specifically target PE to promote this action;[39,109] however, such specificity would seem unlikely to contribute to the action M5-NH_2 against *P. aeruginosa*, given its strong preference for anionic lipid (Table 2). In many cases, the ability of PE to promote the antibacterial action of α-helical AMPs involves the inherent propensity of the lipid's cone shaped molecule to induce negative curvature and non-bilayer structures in membranes.[110,111] This propensity has been shown to contribute to the antibacterial action of α-helical AMPs by promoting a number of membranolytic mechanisms, including the formation of toroidal-type pores and carpet-type modes of action.[45,112–114] In general, each of these mechanisms would fit with the high levels of insertion and lysis found for the action of M5-NH_2 against *P. aeruginosa*, suggesting that similar mechanisms may contribute to this action (Table 2 and Fig. 8). The ability of PE to induce non-bilayer structures also appears to facilitate bacterial membrane destabilization and lysis in response to the oblique insertion of α-helical AMPs that use tilted structure in their antibacterial action.[33,39,67,115–117] This ability would appear to be consistent with the suggestion made above, which was that M5-NH_2 may use tilted mechanisms to promote its membranolytic action against *P. aeruginosa*. Indeed, recent studies have suggested that, in these mechanisms, PE would be key to facilitating the peptide's oblique orientation and ability to perturb membrane properties such as lipid packing and membrane fluidity.[33] The insertion of M5-NH_2 into the CM of *P. aeruginosa* also appeared to lead to the perturbation of these membrane properties, thereby contributing to the peptide's membranolytic action against the organism (Table 2 and Fig. 8D).

As for binding, interactions of M5-NH_2 with anionic lipid in the *P. aeruginosa* CM appeared to drive the remining major steps in the peptide's action against the organism with CL showing the highest levels of α-helicity, insertion and lysis recorded for the peptide (Table 2). However, whilst the levels of α-helicity adopted by the peptide with CL were only around a tenth higher than those with PG, the insertion and lysis shown by M5-NH_2 with CL membranes was over a third higher than those with PG (Table 2). These observations indicated that the peptide adopted comparable levels of α-helicity with these two lipids but showed a much greater ability to penetrate and lyse CL membranes as compared to those formed by PG (Table 2). These data would seem to indicate that CL was the primary driver of α-helix formation, insertion and lysis by M5-NH_2 in its action against *P. aeruginosa* and a number of mechanisms show the potential to support this role for the lipid.

It is well established that CL is able to influence the action of AMPs[98] and in general, this ability derives from the topography of CL, which has a cone shaped molecule that promotes negative membrane curvature, along with the formation of domains and non-bilayer structures.[110,111] This non-lamellar behaviour appears able to inhibit the ability of some α-helical AMPs to insert into bacterial membranes[39,118–120] but in most cases, this behaviour appears to promote mechanisms of membranolytic action by these peptides.[121–129] In general, these mechanisms appear to involve lipid clustering effects where CL is segregated from PE,[125,130,131] which is induced by the strong positive charge of AMPs and appears to be facilitated by the formation of hydrogen bonds between the headgroups of these individual lipid types.[111] In these CL mediated mechanisms, AMPs can either target naturally occurring CL domains or induce these domains in bacterial membranes, which then leads to the bacterial death through membranolytic action, although bacterial killing through non-membranolytic action has been reported.[44,45,121–129,132] For example, a number of α-helical AMPs induce negatively curved CL domains in the CM of *Escherichia coli*,[122] some of which involve clustering,[126,127] to promote non-membranolytic perturbation of this membrane that leads to the lethal disruption of cellular processes.[122,126,127] It is possible that such CL-mediated non-membranolytic mechanisms contribute to the action of M5-NH_2 against *P. aeruginosa*, but, most likely, this contribution would be minor compared to membranolytic mechanisms. Potentially, the non-lamellar behaviour of CL could promote the membranolytic action of M5-NH_2 against *P. aeruginosa* by supporting a number of established models used to describe this action for α-helical AMPs. As examples, α-helical AMPs appear to induce CL domains segregated from PE in the CM of *P. aeruginosa* that promote lysis *via* carpet-like mechanisms,[128,129] and target negatively curved CL domains in the CM of *E. coli* to promote lysis through pore forming mechanisms.[121] It is believed that lipid clustering by α-helical AMPs contributes to carpet-type and pore-forming mechanisms through the production of phase boundary defects that induce leakage in target bacterial membranes.[124,125,132] Based on these observations, it would seem that lipid clustering mechanisms could contribute to the high levels of insertion and lysis found for the action of M5-NH_2 against *P. aeruginosa* (Fig. 8C and D). Indeed, PE is strongly represented in the CM of the organism (Table 1) and M5-NH_2 satisfies the two primary requirements for AMPs that induce lipid clustering effects, namely, a high positive charge and stable secondary structure (Table 2).[123–125,133] Another characteristic of M5-NH_2 that may show the potential to contribute to its CL-mediated membranolytic action against *P. aeruginosa* is its molecular shape; this property is well known to influence the interactions of AMPs with bacterial membranes.[134] The molecular shape of M5-NH_2 is formed by a large hydrophilic surface and a smaller hydrophobic surface, resembling an inverted cone (Fig. 1). Synthetic AMPs with a similar molecular shape to M5-NH_2 appeared to kill *P. aeruginosa* by complementing the cone shape of CL, thereby promoting an increase in CM tension that resulted in pore formation and other effects that led to cell death.[135–137] Interestingly, CL is also present in the OM of Gram-negative bacteria[138] and in the case of *E. coli*, α-helical AMPs have been to promote lysis of this membrane *via* carpet-like mechanisms using CL mediated clustering effects.[121] These mechanisms appeared to make only a minor contribution to the overall membranolytic action of these AMPs, but it is possible that similar mechanisms could contribute to the action of M5-NH_2 against *P. aeruginosa*.[121]

M5-NH_2 showed weak activity against *S. aureus* that was in the hundred micromolar range, which indicated resistance to the action of the peptide and was in strong contrast to its potent action against *P. aeruginosa* and other Gram-positive bacteria (Fig. S1; Table 2, ESI†).[33] The *S. aureus* CM shows major differences in lipid composition to those of *P. aeruginosa* (Table 1) and such differences are well known to play a role in determining the specificity, susceptibility, and resistance of AMPs for bacteria.[39,45,107,109] Here, these differences appeared to mediate the resistance of *S. aureus* to the action of M5-NH_2 by decreasing the peptide's capacity for membranolytic action (Table 2). To gain insight into mechanisms underpinning this resistance, individual, major steps in the interaction of M5-NH_2 with the CM of *S. aureus* were studied and a synthesis of these data allowed a putative scheme for the action of the peptide against the organism to be constructed (Fig. 9).

In the first major step of its action against *S. aureus*, M5-NH_2 shows weak binding to the CM of the organism (Fig. 10A) that is orders of magnitude lower than that in the case of *P. aeruginosa* (Table 2). The CM of *S. aureus* contrasts to that of *P. aeruginosa* in that it possesses *circa* a two-fold higher content of anionic lipid which is predominantly formed from PG rather than CL (Table 1). This would seem to indicate that PG primarily drives the binding of M5-NH_2 to the CM of *S. aureus* and that the peptide's lower affinity for this lipid relative to CL could contribute to the weaker binding of the peptide as compared to that in the case of *P. aeruginosa* (Table 2 and Fig. 8A). However, the major difference between the lipid compositions of the CM of *S. aureus* and *P. aeruginosa* is the presence of the positively charged lipid Lys-PG in the CM of the former organism (Table 1). It is well established that the high levels of the lipid in these membranes reduce the overall negative charge of CL and PG, which leads to the electrostatic repulsion of AMPs and effectively lowers their ability to bind these membranes.[71,72,139,140] This ability is consistent with the differing levels of bacterial membrane affinity shown here by M5-NH_2 and strongly suggests that similar Lys-PG-mediated electrostatic effects underpin the weak binding of the peptide to the CM of *S. aureus* (Table 2). Taken in combination, these data strongly suggest that the Lys-PG-mediated attenuation of membrane binding makes a major contribution to reducing the membranolytic efficacy of M5-NH_2, thereby promoting the resistance of *S. aureus* to the action of the peptide (Fig. 10A) In support of this suggestion, Lys-PG has also been detected in the CM of other bacteria[55,139–141] and appears to inhibit binding by AMPs in resistance mechanism with similarities to that mediated by the lipid in *S. aureus*.[55,71,142–148] Interestingly, in what seems to be an evolutionary response, some creatures appear to produce anionic AMPs that bind Lys-PG to overcome *S. aureus* resistance mechanisms and promote their antibacterial action.[149]

The weak affinity of M5-NH_2 for the CM of *S. aureus* appeared to limit rather than completely abolish the ability of the peptide to interact with these membranes. In the next two major steps of this interaction, M5-NH_2 showed low levels of α-helicity and insertion with the CM of *S. aureus* (Fig. 9B) that were around one half of those shown by the peptide with that from *P. aeruginosa* (Table 2). This relative decrease in the efficacy of M5-NH_2 to perform these steps appeared to be mediated by the presence of Lys-PG in the CM of *S. aureus* (Fig. 9B). In the case of α-helix formation by the peptide, it is known that the positive charge on Lys-PG is able to influence the energy barrier for the adoption of this structure by AMPs and this ability appears to primarily depend on the charge carried by these peptides.[38,68,69] Studies on anionic α-helical AMPs with action against *S. aureus*, showed that Lys-PG has no effect on the levels of α-helical structure adopted by these peptides.[38] In this case, it appeared that electrostatic interactions between negatively charged residues in these AMPs and the lipid neutralised its ability to influence their conformational behaviour.[38] In contrast, studies on strongly cationic α-helical AMPs resisted by *S. aureus* reported that electrostatic repulsion between these peptides and Lys-PG in the organism's membranes inhibited the process of α-helix formation by these AMPs.[68,69] These electrostatic repulsion effects appeared to raise the energy barrier for this process and counter the ability of CL and PG in the *S. aureus* CM to induce α-helical structure in these AMPs.[68,69] Taken in combination, these observations strongly suggest that, in its action against *S. aureus*, Lys-PG mediated electrostatic effects inhibit the ability of M5-NH_2 to adopt the higher levels of α-helicity seen with *P. aeruginosa*, thereby promoting the resistance of *S. aureus* to the peptide (Table 2 and Fig. 10B).

Lys-PG-mediated reductions in the α-helicity of M5-NH_2 also appeared to promote the resistance of *S. aureus* to the peptide by decreasing its efficacy in the step of insertion into the organism's CM (Fig. 10C). In this step, the lower α-helicity of M5-NH_2 led to levels of insertion into the *S. aureus* CM that were more associated with their head-group and upper regions than the deep penetration of their hydrophobic core seen with *P. aeruginosa* (Fig. 10C). Clearly, a major potential contributor to these decreased levels of insertion would seem to be the loss of amphiphilic structure associated with reduced α-helix formation by M5-NH_2, given that, as suggested above, amphiphilicity appears to drive the peptide's membrane interactions. Another potential contributor to these decreased levels of insertion could be disruption of the peptide's hydrophobicity gradient resulting from its lower adoption of α-helical structure, as compared to the case of *P. aeruginosa*. Indeed, the tilted insertion of M5-NH_2 into the *S. aureus* CM could be further compromised by their lack of PE (Table 1) and the ability of the lipid's non-lamellar behaviour to facilitate this form of bilayer penetration.[33,39,67,115–117] Reduced insertion into the *S. aureus* CM due to Lys-PG-mediated decreased α-helicity in M5-NH_2 (Table 2 and Fig. 9B) could also contribute to *S. aureus* resistance by inhibiting the use of novel anionic clustering mechanisms reported for the action of AMPs against Gram-positive bacteria. In these clustering mechanisms, strongly cationic AMPs promote their antibacterial action through membrane perturbation involving the induced segregation of CL from PG.[123,125] However, the low levels of α-helicity shown by M5-NH_2 with the *S. aureus* CM (Table 2 and Fig. 9B) would appear to lie outside the conformational requirements of lipid clustering mechanisms, rendering their use by the peptide in this case unlikely.[123–125,133] In addition to mechanisms

involving Lys-PG-mediated changes to the conformational behaviour of M5-NH_2, the insertion of the peptide into the *S. aureus* CM could also be limited by mechanisms based on the intrinsic properties of the lipid itself. It has previously been shown that the ability of Lys-PG to reduce electrostatic repulsion between CL and PG lipid head-groups leads to decreases in the fluidity of the *S. aureus* CM[70,150] and makes partitioning by AMPs more difficult.[72,73,141,151,152]

In the major steps discussed above, it was suggested that Lys-PG promoted the resistance of *S. aureus* to M5-NH_2 by reducing the peptide's capacity for membranolytic action and that a number of mechanisms mediated by the lipid could potentially promote these effects (Fig. 10D). Strongly supporting this suggestion, in the final major step of this action, the membranolytic capacity of M5-NH_2 against *S. aureus* was around one third of that shown against *P. aeruginosa* (Table 2) and this decreased membranolytic efficacy appeared to be mediated by Lys-PG (Fig. 9). Taken in combination, the Lys-PG-mediated effects found for steps in the action of M5-NH_2 against *S. aureus* (Table 2 and Fig. 10) are consistent with those of a major intrinsic mechanism used by the organism to resist AMPs.[72,151,153] This mechanism is modulated by the MprF operon and involves the catalytic lysylination of PG to produce Lys-PG, which is subsequently translocated to the outer leaflet of *S. aureus* membranes.[140,154]

Although Lys-PG-mediated reductions in membranolytic efficacy clearly appeared to be a major driver in the resistance of *S. aureus* to the action of M5-NH_2, the peptide showed a weak ability to induce the lysis of the organism's membranes. This effect could reflect the fact that the *in vivo* situation of *S. aureus* membranes is not fully represented by the *in vitro* membrane systems used in the present study. One explanation for these observations is that other mechanisms play a minor role in the resistance of *S. aureus* to the action of M5-NH_2 and it is well established that the organism uses a variety of strategies to resist AMPs.[44,151,155] A frequently reported strategy would involve interactions between M5-NH_2 and components of the *S. aureus* cell wall when the peptide was migrating to the organism's CM. The *S. aureus* cell wall can be considered as essentially a thick peptidoglycan (PGN) mesh that is decorated with anionic teichoic acids.[156] In general, PGN appears to not significantly hinder the passage of AMPs as it is not anionic and is porous to molecules with molecular weights that would include M5-NH_2 and most AMPs.[44,157–159] However, the D-alanylation of teichoic acids to decrease their negative charge and promote electrostatic repulsion effects with AMPs is known to inhibit the access of these peptides to *S. aureus* membranes.[44,158–160] Very recent studies have suggested that this access is also restricted by modifications to the polymer composition and/or synthesis of teichoic acids anchored to these membranes. These modifications appear to be modulated by MprF and function with Lys-PG electrostatic repulsion effects and teichoic acid D-alanylation to decrease the overall permeability of the *S. aureus* cell wall to AMPs.[161]

Conclusions

M5-NH_2, was designed to exhibit broad antimicrobial activity[26,27] and shows potent action against a spectrum of fungi and bacteria,[26,27,30–33] although the mechanisms underpinning this action has been investigated in only a few cases, which has been extended in the present study.[31–33] The peptide showed potent membranolytic activity against *P. aeruginosa* (Fig. S1 and Table 2, ESI†) and similar results have been reported for the activity of M5-NH_2 against *E. coli*,[31,32] which is increasingly regarded as an ESKAPE pathogen.[35] These observations suggested that the peptide may have broad range action against Gram-negative bacteria and the potential to kill not only *P. aeruginosa* and *E. coli* but also other ESKAPE pathogens such as *K. pneumoniae*.[162] However, although M5-NH_2 showed potent membranolytic action against *B subtilis*,[33] *S. aureus* was resistant to the peptide (Fig. S1 and Table 2, ESI†) using mechanisms available to other Gram-positive bacteria, clearly suggesting that the peptide's activity against these bacteria may show a more limited spectrum.[55,71,142–148]

Characterisation of the antibacterial activity of M5-NH_2 showed it to possess potent CL driven membranolytic action against *P. aeruginosa* but was rendered ineffective against *S. aureus* by Lys-PG driven inhibition of this action (Table 2). These observations clearly showed the effect of differences in the lipid compositions of bacterial membranes on the activity of AMPs and reinforce the importance of taking these differences into account when designing these peptides.[163] Indeed, it has been recently suggested that when designing AMPs, other often neglected factors, such as site of action pH should also be considered;[164,165] changes in pH have been shown to both enhance and attenuate the response of *S. aureus* and *P. aeruginosa* to the action of AMPs.[38,39,76]

The Lys-PG mediated mechanisms shown here to protect *S. aureus* to the action of M5-NH_2 most probably involve the use of an intrinsic resistance mechanism frequently reported in studies on the susceptibility of the organism to AMPs.[72,151,153] The use of this intrinsic mechanism to resist M5-NH_2, as opposed to those that are acquired,[166] would help to explain the fact that many other strains of *S. aureus* show similar levels of resistance to the action of the peptide.[27] Indeed, *S. aureus*, particularly MRSA, shows resistance to many AMPs, which has hindered progress in the development of these peptides as therapeutic agents to combat infections due to the organism.[44,83,151,155] In part, this lack of progress has been due to a poor understanding of the mechanisms used by *S. aureus* to resist the action of AMPs and why these mechanisms work against some of these peptides and not others. It is well known that some AMPs with a similar charge to M5-NH_2 are able to kill *S. aureus*, whilst others are resisted by the organism using Lys-PG mediated mechanisms.[167] It is to be hoped that the data presented here will help to explain these differences and increase the general understanding of mechanisms underpinning the ability of *S. aureus* to resist AMPs.

Potentially, the CL driven membranolytic activity of M5-NH_2 against *P. aeruginosa* involved the peptide's ability to adopt tilted α-helical structure and induce anionic lipid clustering. These mechanisms were consistent with the overall effects of the peptide's membranolytic action against *P. aeruginosa* and a number of models appeared able to describe this action,

including toroidal-type pore formation and carpet-type mechanisms. In carpet-type mechanisms, AMPs promote their antibacterial activity using a detergent-like membranolytic action that does not generally entail the penetration of these peptide into the CM hydrophobic core region.[10,11] In contrast, the use of toroidal pore formation to promote antibacterial membranolytic action by AMPs generally involves deep penetration of the bacterial CM.[14,15] Given the ability of M5-NH_2 to penetrate and perturb the acyl chain region of the *P. aeruginosa* CM, this might suggest that the peptide is more likely to use toroidal-type mechanisms than carpet-type mechanisms. Based on its action against *P. aeruginosa* and lack of haemolytic activity,[28] M5-NH_2 shows the potential for medical development in a number of areas,[168,169] including biofilm inhibition[170] combination therapy[171] and cystic fibrosis treatment.[172]

Author contributions

S. R. D., F. H. and D. A. P. designed the research. K. B. synthesised the peptide. S. R. D. and L. H. G. M. performed research. S. R. D., L. H. G. M. and F. H. analysed data. S. R. D., L. H. G. M, K. B. F. H. and D. A. P. wrote the manuscript.

Conflicts of interest

The authors declare no conflict of interest.

Acknowledgements

The peptide M5-NH_2 (KLAKKLAKLAKLAKALCONH$_2$) was partially funded by the Biochemical Society Eric Reid Fund for Methodology.

References

1 J. O'Neill, 2016. Tackling drug-resistant infections globally: final report and recommendations. **https://amr-review.org/sites/default/files/160518_Final%20paper_with%20cover.pdf**.
2 M. E. de Kraker, A. J. Stewardson and S. Harbarth, *PLoS Med.*, 2016, **13**, e1002184.
3 M. Terreni, M. Taccani and M. Pregnolato, *Molecules*, 2021, 26.
4 T. M. Uddin, A. J. Chakraborty, A. Khusro, B. M. R. M. Zidan, S. Mitra, T. B. Emran, K. Dhama, M. K. H. Ripon, M. Gajdács, M. U. K. Sahibzada, M. J. Hossain and N. Koirala, *J. Infection Public Health*, 2021, **14**, 1750–1766.
5 D. M. P. De Oliveira, B. M. Forde, T. J. Kidd, P. N. A. Harris, M. A. Schembri, S. A. Beatson, D. L. Paterson and M. J. Walker, *Clin. Microbiol. Rev.*, 2020, **33**, e00181-19.
6 G. Mancuso, A. Midiri, E. Gerace and C. Biondo, *Pathogens*, 2021, **10**, 1310.
7 X. Zhen, C. S. Lundborg, X. Sun, X. Hu and H. Dong, *Antimicrobial Resistance Infection Control*, 2019, **8**, 137.
8 M. Rima, M. Rima, Z. Fajloun, J. M. Sabatier, B. Bechinger and T. Naas, *Antibiotics*, 2021, **10**, 1095.
9 Y.-X. Ma, C.-Y. Wang, Y.-Y. Li, J. Li, Q.-Q. Wan, J.-H. Chen, F. R. Tay and L.-N. Niu, *Adv. Sci.*, 2020, **7**, 1901872.
10 Q.-Y. Zhang, Z.-B. Yan, Y.-M. Meng, X.-Y. Hong, G. Shao, J.-J. Ma, X.-R. Cheng, J. Liu, J. Kang and C.-Y. Fu, *Military Med. Res.*, 2021, **8**, 48.
11 S. Li, Y. Wang, Z. Xue, Y. Jia, R. Li, C. He and H. Chen, *Trends Food Sci. Technol.*, 2021, **109**, 103–115.
12 M. Abdi, S. Mirkalantari and N. Amirmozafari, *J. Pept. Sci.*, 2019, **25**, e3210.
13 R. Nuri, T. Shprung and Y. Shai, *Biochim. Biophys. Acta, Biomembr.*, 2015, **1848**, 3089–3100.
14 G. Wang, A. Verma and S. Reiling, in *Antimicrobial Peptides*, ed. K. Ajesh and K. Sreejith, Academic Press, 2023, pp. 237–259, DOI: **10.1016/B978-0-323-85682-9.00012-X**.
15 T. Rončević, J. Puizina and A. Tossi, *Int. J. Mol. Sci.*, 2019, **20**, 5713.
16 A. Pfalzgraff, K. Brandenburg and G. Weindl, *Front. Pharmacol.*, 2018, **9**, 281.
17 M. S. Mulani, E. E. Kamble, S. N. Kumkar, M. S. Tawre and K. R. Pardesi, *Front. Microbiol.*, 2019, **10**, 539.
18 S. Mukhopadhyay, A. S. Bharath Prasad, C. H. Mehta and U. Y. Nayak, *World J. Microbiol. Biotechnol.*, 2020, **36**, 131.
19 A. Parchebafi, F. Tamanaee, H. Ehteram, E. Ahmad, H. Nikzad and H. Haddad Kashani, *Microb. Cell Fact.*, 2022, **21**, 118.
20 G. S. Dijksteel, M. M. W. Ulrich, E. Middelkoop and B. Boekema, *Front. Microbiol.*, 2021, **12**, 616979.
21 M. Lesiuk, M. Paduszyńska and K. E. Greber, *Antibiotics*, 2022, **11**, 1062.
22 G. Wang and A. F. Mechesso, *Admet dmpk*, 2022, **10**, 91–105.
23 B. H. Gan, J. Gaynord, S. M. Rowe, T. Deingruber and D. R. Spring, *Chem. Soc. Rev.*, 2021, **50**, 7820–7880.
24 S.-J. Kang, S. H. Nam and B.-J. Lee, *Antibiotics*, 2022, **11**, 1338.
25 P. G. Lima, J. T. A. Oliveira, J. L. Amaral, C. D. T. Freitas and P. F. N. Souza, *Life Sci.*, 2021, **278**, 119647.
26 R. Bessalle, A. Gorea, I. Shalit, J. W. Metzger, C. Dass, D. M. Desiderio and M. Fridkin, *J. Med. Chem.*, 1993, **36**, 1203–1209.
27 D. R. Owen, 2005. Short bioactive peptides. Helix Biomedix Inc: USA. The full form of this is Owen DR (2005) Short bioactive peptides in, Helix BioMedix. Inc., USA. United States Patent 6875744.**https://patents.google.com/patent/US6875744B2/en**.
28 S. R. Dennison and D. A. Phoenix, *Eur. Biophys. J.*, 2014, **43**, 423–432.
29 S. R. Dennison, F. Harris, T. Bhatt, J. Singh and D. A. Phoenix, *Mol. Cell. Biochem.*, 2009, **333**, 129.
30 S. R. Dennison, F. Harris, T. Bhatt, J. Singh and D. A. Phoenix, *Mol. Cell. Biochem.*, 2009, **332**, 43.
31 S. Dennison and D. Phoenix, *Biochemistry*, 2011, **50**, 1514–1523.
32 S. R. Dennison and D. A. Phoenix, *Biochemistry*, 2011, **50**, 10898–10909.
33 S. R. Dennison, T. Haußß, K. Badiani, F. Harris and D. A. Phoenix, *Soft Matter*, 2019, **15**, 4215–4226.

34 H. Venter, *Biosci. Rep.*, 2019, **39**, BSR20180474.
35 J. Denissen, B. Reyneke, M. Waso-Reyneke, B. Havenga, T. Barnard, S. Khan and W. Khan, *Int. J. Hyg. Environ. Health*, 2022, **244**, 114006.
36 F. Savini, S. Bobone, D. Roversi, M. L. Mangoni and L. Stella, *Pept. Sci.*, 2018, **110**, e24041.
37 M. Rojewska, W. Smułek, E. Kaczorek and K. Prochaska, *Membranes*, 2021, **11**, 707.
38 S. R. Dennison, L. H. Morton, F. Harris and D. A. Phoenix, *Biochemistry*, 2016, **55**, 3735–3751.
39 E. Malik, D. A. Phoenix, K. Badiani, T. J. Snape, F. Harris, J. Singh, L. H. G. Morton and S. R. Dennison, *Biochim. Biophys. Acta, Biomembr.*, 2020, **1862**, 183141.
40 S. R. Dennison, F. Harris and D. A. Phoenix, *Protein Pept. Lett.*, 2010, **17**, 1363–1375.
41 S. R. Dennison, F. Harris and D. A. Phoenix, in *Advances in Planar Lipid Bilayers and Liposomes*, ed. A. Iglič and C. V. Kulkarni, Academic Press, 2014, vol. 20, pp. 83–110.
42 C. Wölk, H. Youssef, T. Guttenberg, H. Marbach, G. Vizcay-Barrena, C. Shen, G. Brezesinski and R. D. Harvey, *ChemPhysChem*, 2020, **21**, 702–706.
43 S. Danner, G. Pabst, K. Lohner and A. Hickel, *Biophys. J.*, 2008, **94**, 2150–2159.
44 N. Malanovic and K. Lohner, *Biochim. Biophys. Acta*, 2016, **1858**, 936–946.
45 V. Teixeira, M. J. Feio and M. Bastos, *Prog. Lipid Res.*, 2012, **51**, 149–177.
46 P. J. O'Toole, I. E. Morrison and R. J. Cherry, *Biochim. Biophys. Acta*, 2000, **1466**, 39–46.
47 J. Wall, C. A. Golding, M. Van Veen and P. O'Shea, *Mol. Membr. Biol.*, 1995, **12**, 183–192.
48 A. J. Miles, S. G. Ramalli and B. A. Wallace, *Protein Sci.*, 2022, **31**, 37–46.
49 J. Todd, *Introduction to the Constructive Theory of Functions*, Academic Press, 1963.
50 R. Gautier, D. Douguet, B. Antonny and G. Drin, *Bioinformatics*, 2008, **24**, 2101–2102.
51 M. J. McKay, F. Afrose, R. E. Koeppe, 2nd and D. V. Greathouse, *Biochim. Biophys. Acta, Biomembr.*, 2018, **1860**, 2108–2117.
52 Y. He and T. Lazaridis, *PLoS One*, 2013, **8**, e66440.
53 C. I. von Deuster and V. Knecht, *Biochim. Biophys. Acta*, 2012, **1818**, 2192–2201.
54 A. Catte, M. R. Wilson, M. Walker and V. S. Oganesyan, *Soft Matter*, 2018, **14**, 2796–2807.
55 C. Sohlenkamp and O. Geiger, *FEMS Microbiol. Rev.*, 2015, **40**, 133–159.
56 O. G. Travkova, H. Moehwald and G. Brezesinski, *Adv. Colloid Interface Sci.*, 2017, **247**, 521–532.
57 D. A. Phoenix and F. Harris, *Mol. Membr. Biol.*, 2002, **19**, 1–10.
58 D. A. Phoenix, F. Harris, O. A. Daman and J. Wallace, *Curr. Protein Pept. Sci.*, 2002, **3**, 201–221.
59 Q. Wang, B. Peng, M. Song, Abdullah, J. Li, J. Miao, K. Feng, F. Chen, X. Zhai and Y. Cao, *Front. Nutrition*, 2021, **8**, DOI: **10.3389/fnut.2021.768890**.
60 A. Morales-Martínez, B. Bertrand, J. M. Hernández-Meza, R. Garduño-Juárez, J. Silva-Sanchez and C. Munoz-Garay, *Biophys. J.*, 2022, **121**, 3034–3048.
61 B. Zorilă, G. Necula, M. Radu and M. Bacalum, *Toxins*, 2020, **12**, 705.
62 S. Omardien, J. W. Drijfhout, F. M. Vaz, M. Wenzel, L. W. Hamoen, S. A. Zaat and S. Brul, *Biochim. Biophys. Acta, Biomembr.*, 2018, **1860**, 2404–2415.
63 S. Qian and P. A. Zolnierczuk, *BBA Adv*, 2022, **2**, 100045.
64 Y. Shai, *Pept. Sci.*, 2002, **66**, 236–248.
65 W. Im and C. L. Brooks, 3rd, *Proc. Natl. Acad. Sci. U. S. A.*, 2005, **102**, 6771–6776.
66 S. R. Dennison, L. H. G. Morton and D. A. Phoenix, *Biochim. Biophys. Acta, Biomembr.*, 2012, **1818**, 2094–2102.
67 S. R. Dennison, L. H. Morton, F. Harris and D. A. Phoenix, *Chem. Phys. Lipids*, 2008, **151**, 92–102.
68 P. W. Simcock, M. Bublitz, F. Cipcigan, M. G. Ryadnov, J. Crain, P. J. Stansfeld and M. S. P. Sansom, *bioRxiv*, 2020, DOI: **10.1101/2020.04.24.057349**.
69 R. Rehal, R. D. Barker, Z. Lu, T. T. Bui, B. Demé, G. Hause, C. Wölk and R. D. Harvey, *Biochim. Biophys. Acta, Biomembr.*, 2021, **1863**, 183571.
70 E. Kilelee, A. Pokorny, M. R. Yeaman and A. S. Bayer, *Antimicrob. Agents Chemother.*, 2010, **54**, 4476–4479.
71 W. R. Miller, A. S. Bayer and C. A. Arias, *Cold Spring Harbor Perspect. Med.*, 2016, **6**, a026997.
72 C. M. Ernst and A. Peschel, *Int. J. Med. Microbiol.*, 2019, **309**, 359–363.
73 T. Shireen, M. Singh, T. Das and K. Mukhopadhyay, *Antimicrob. Agents Chemother.*, 2013, **57**, 5134–5137.
74 J. A. den Kamp, I. Redai and L. L. van Deenen, *J. Bacteriol.*, 1969, **99**, 298–303.
75 J. R. Willdigg and J. D. Helmann, *Front. Mol. Biosci.*, 2021, **8**, DOI: **10.3389/fmolb.2021.634438**.
76 R. Rehal, P. R. J. Gaffney, A. T. M. Hubbard, R. D. Barker and R. D. Harvey, *Eur. J. Pharm. Sci.*, 2019, **128**, 43–53.
77 A. J. Kunz Coyne, A. El Ghali, D. Holger, N. Rebold and M. J. Rybak, *Infectious Diseases Therapy*, 2022, **11**, 661–682.
78 M. Vestergaard, D. Frees and H. Ingmer, *Microbiol. Spectrosc.*, 2019, **7**, DOI: **10.1128/microbiolspec.GPP3-0057-2018**.
79 E. V. K. Ledger, A. Sabnis and A. M. Edwards, *Microbiology*, 2022, **168**, DOI: **10.1099/mic.0.001136**.
80 S. Ruden, A. Rieder, T. Schwartz, R. Mikut and K. Hilpert, *bioRxiv*, 2019, DOI: **10.1101/639286**, 639286.
81 A. J. Mulkern, L. B. Oyama, A. R. Cookson, C. J. Creevey, T. J. Wilkinson, H. Olleik, M. Maresca, G. C. da Silva, P. P. Fontes, D. M. S. Bazzolli, H. C. Mantovani, B. F. Damaris, L. A. J. Mur and S. A. Huws, *npj Biofilms Microbiomes*, 2022, **8**, 70.
82 A. Mazumdar and V. Adam, *JMCM*, 2021, **4**, 1–17.
83 A. Zouhir, T. Jridi, A. Nefzi, J. Ben Hamida and K. Sebei, *Pharm. Biol.*, 2016, **54**, 3136–3150.
84 E. B. Breidenstein, C. de la Fuente-Núñez and R. E. Hancock, *Trends Microbiol.*, 2011, **19**, 419–426.
85 J. Ude, V. Tripathi, J. M. Buyck, S. Söderholm, O. Cunrath, J. Fanous, B. Claudi, A. Egli, C. Schleberger, S. Hiller and

D. Bumann, *Proc. Natl. Acad. Sci. U. S. A.*, 2021, **118**, DOI: 10.1073/pnas.2107644118.
86 J. D. Prajapati, U. Kleinekathöfer and M. Winterhalter, *Chem. Rev.*, 2021, **121**, 5158–5192.
87 A. H. Delcour, *Biochim. Biophys. Acta*, 2009, **1794**, 808–816.
88 P. Sharma and K. G. Ayappa, *J. Membr. Biol.*, 2022, **255**, 665–675.
89 A. Barreto-Santamaría, G. Arévalo-Pinzón, M. A. Patarroyo and M. E. Patarroyo, *Antibiotics*, 2021, **10**, 1499.
90 N. Klubthawee, P. Adisakwattana, W. Hanpithakpong, S. Somsri and R. Aunpad, *Sci. Rep.*, 2020, **10**, 9117.
91 M. Yasir, D. Dutta and M. D. P. Willcox, *Sci. Rep.*, 2019, **9**, 7063.
92 H. Chai, W. E. Allen and R. P. Hicks, *Int. J. Med. Chem.*, 2014, **2014**, 809283.
93 L. Zhang, P. Dhillon, H. Yan, S. Farmer and R. E. Hancock, *Antimicrob. Agents Chemother.*, 2000, **44**, 3317–3321.
94 M. Sathappa and N. N. Alder, *Biochim. Biophys. Acta, Biomembr.*, 2016, **1858**, 1362–1372.
95 H. I. MacDermott-Opeskin, V. Gupta and M. L. O'Mara, *Biophys. Rev.*, 2022, **14**, 145–162.
96 P. F. Almeida, A. S. Ladokhin and S. H. White, *Biochim. Biophys. Acta, Biomembr.*, 2012, **1818**, 178–182.
97 M. E. Fealey, B. P. Binder, V. N. Uversky, A. Hinderliter and D. D. Thomas, *Biophys. J.*, 2018, **114**, 550–561.
98 R. N. Lewis and R. N. McElhaney, *Biochim. Biophys. Acta, Biomembr.*, 2009, **1788**, 2069–2079.
99 F. Harris, A. Daman, J. Wallace, S. R. Dennison and D. A. Phoenix, *Curr. Protein Pept. Sci.*, 2006, **7**, 529–537.
100 D. Juretić and J. Simunić, *Expert Opin. Drug Discovery*, 2019, **14**, 1053–1063.
101 X. Zhu, N. Dong, Z. Wang, Z. Ma, L. Zhang, Q. Ma and A. Shan, *Acta Biomater.*, 2014, **10**, 244–257.
102 J. Wang, S. Chou, Z. Yang, Y. Yang, Z. Wang, J. Song, X. Dou and A. Shan, *J. Med. Chem.*, 2018, **61**, 3889–3907.
103 X. Chen, S. Ji, A. Li, H. Liu and H. Fei, *J. Med. Chem.*, 2020, **63**, 1132–1141.
104 F. Harris, J. Wallace and D. A. Phoenix, *Mol. Membr. Biol.*, 2000, **17**, 201–207.
105 M. Mura, S. R. Dennison, A. V. Zvelindovsky and D. A. Phoenix, *Biochim. Biophys. Acta, Biomembr.*, 2013, **1828**, 586–594.
106 S. R. Dennison, F. Harris and D. A. Phoenix, *Protein Pept. Lett.*, 2005, **12**, 27–29.
107 D. A. Phoenix, F. Harris, M. Mura and S. R. Dennison, *Prog. Lipid Res.*, 2015, **59**, 26–37.
108 S. R. Dennison, F. Harris, M. Mura, L. H. G. Morton, A. Zvelindovsky and D. A. Phoenix, *Biochemistry*, 2013, **52**, 6021–6029.
109 H. Schröder-Borm, R. Willumeit, K. Brandenburg and J. Andrä, *Biochim. Biophys. Acta, Biomembr.*, 2003, **1612**, 164–171.
110 J. Jouhet, *Front. Plant Sci.*, 2013, **4**, 494.
111 K. Matsumoto, J. Kusaka, A. Nishibori and H. Hara, *Mol. Microbiol.*, 2006, **61**, 1110–1117.
112 R. Willumeit, M. Kumpugdee, S. S. Funari, K. Lohner, B. P. Navas, K. Brandenburg, S. Linser and J. Andrä, *Biochim. Biophys. Acta, Biomembr.*, 2005, **1669**, 125–134.
113 D. J. Paterson, M. Tassieri, J. Reboud, R. Wilson and J. M. Cooper, *Proc. Natl. Acad. Sci. U. S. A.*, 2017, **114**, E8324–E8332.
114 E. F. Haney, S. Nathoo, H. J. Vogel and E. J. Prenner, *Chem. Phys. Lipids*, 2010, **163**, 82–93.
115 L. Lins, M. Decaffmeyer, A. Thomas and R. Brasseur, *Biochim. Biophys. Acta, Biomembr.*, 2008, **1778**, 1537–1544.
116 S. R. Dennison, L. H. G. Morton, K. Brandenburg, F. Harris and D. A. Phoenix, *FEBS J.*, 2006, **273**, 3792–3803.
117 L. Lins and R. Brasseur, *J. Pept. Sci.*, 2008, **14**, 416–422.
118 D. Poger, S. Pöyry and A. E. Mark, *ACS Omega*, 2018, **3**, 16453–16464.
119 L. Hernández-Villa, M. Manrique-Moreno, C. Leidy, M. Jemioła-Rzemińska, C. Ortíz and K. Strzałka, *Biophys. Chem.*, 2018, **238**, 8–15.
120 N. Calderón-Rivera, J. Múnera-Jaramillo, S. Jaramillo-Berrio, E. Suesca, M. Manrique-Moreno and C. Leidy, *Membranes*, 2023, **13**, 304.
121 N. Rangarajan, S. Bakshi and J. C. Weisshaar, *Biochemistry*, 2013, **52**, 6584–6594.
122 M. Makowski, M. R. Felício, I. C. M. Fensterseifer, O. L. Franco, N. C. Santos and S. Gonçalves, *Int. J. Mol. Sci.*, 2020, **21**, 9104.
123 R. F. Epand, L. Maloy, A. Ramamoorthy and R. M. Epand, *Biophys. J.*, 2010, **98**, 2564–2573.
124 R. F. Epand, W. L. Maloy, A. Ramamoorthy and R. M. Epand, *Biochemistry*, 2010, **49**, 4076–4084.
125 R. M. Epand, in *Antimicrobial Peptides: Basics for Clinical Application*, ed. K. Matsuzaki, Springer Singapore, Singapore, 2019, pp. 65–71, DOI: 10.1007/978-981-13-3588-4_5.
126 D. Zweytick, G. Deutsch, J. Andrä, S. E. Blondelle, E. Vollmer, R. Jerala and K. Lohner, *J. Biol. Chem.*, 2011, **286**, 21266–21276.
127 D. Zweytick, B. Japelj, E. Mileykovskaya, M. Zorko, W. Dowhan, S. E. Blondelle, S. Riedl, R. Jerala and K. Lohner, *PLoS One*, 2014, **9**, e90228.
128 L. Lombardi, M. I. Stellato, R. Oliva, A. Falanga, M. Galdiero, L. Petraccone, G. D'Errico, A. De Santis, S. Galdiero and P. Del Vecchio, *Sci. Rep.*, 2017, **7**, 44425.
129 Y. K. Cherniavskyi, R. Oliva, M. Stellato, P. D. Vecchio, S. Galdiero, A. Falanga, S. A. Dames and D. P. Tieleman, *bioRxiv*, 2021, DOI: 10.1101/2021.03.30.437760.
130 R. M. Epand and R. F. Epand, *Biochim. Biophys. Acta*, 2009, **1788**, 289–294.
131 R. M. Epand, S. Rotem, A. Mor, B. Berno and R. F. Epand, *J. Am. Chem. Soc.*, 2008, **130**, 14346–14352.
132 R. M. Epand and R. F. Epand, *J. Pept. Sci.*, 2011, **17**, 298–305.
133 P. Wadhwani, R. F. Epand, N. Heidenreich, J. Bürck, A. S. Ulrich and R. M. Epand, *Biophys. J.*, 2012, **103**, 265–274.
134 B. Bechinger, *Curr. Opin. Colloid Interface Sci.*, 2009, **14**, 349–355.
135 G. Sautrey, M. El Khoury, A. G. Dos Santos, L. Zimmermann, M. Deleu, L. Lins, J.-L. Décout and M.-P. Mingeot-Leclercq, *J. Biol. Chem.*, 2016, **291**, 13864–13874.
136 M. El Khoury, J. Swain, G. Sautrey, L. Zimmermann, P. Van Der Smissen, J.-L. Décout and M.-P. Mingeot-Leclercq, *Sci. Rep.*, 2017, **7**, 10697.

137 J. Swain, M. El Khoury, J. Kempf, F. Briée, P. Van Der Smissen, J. L. Décout and M. P. Mingeot-Leclercq, *PLoS One*, 2018, **13**, e0201752.
138 J. E. Horne, D. J. Brockwell and S. E. Radford, *J. Biol. Chem.*, 2020, **295**, 10340–10367.
139 C. M. Ernst and A. Peschel, *Mol. Microbiol.*, 2011, **80**, 290–299.
140 G. Panda, S. Dash and S. K. Sahu, *Membranes*, 2022, 12.
141 H. Roy, *IUBMB Life*, 2009, **61**, 940–953.
142 Y. Ramos, S. Sansone, S. M. Hwang, T. A. Sandoval, M. Zhu, G. Zhang, J. R. Cubillos-Ruiz and D. K. Morales, *mBio*, 2022, **13**, e0229422.
143 Y. Bao, T. Sakinc, D. Laverde, D. Wobser, A. Benachour, C. Theilacker, A. Hartke and J. Huebner, *PLoS One*, 2012, **7**, e38458.
144 S. Samant, F. F. Hsu, A. A. Neyfakh and H. Lee, *J. Bacteriol.*, 2009, **191**, 1311–1319.
145 E. Maloney, D. Stankowska, J. Zhang, M. Fol, Q. J. Cheng, S. Lun, W. R. Bishai, M. Rajagopalan, D. Chatterjee and M. V. Madiraju, *PLoS Pathog.*, 2009, **5**, e1000534.
146 C. Sohlenkamp, K. A. Galindo-Lagunas, Z. Guan, P. Vinuesa, S. Robinson, J. Thomas-Oates, C. R. Raetz and O. Geiger, *Mol Plant Microbe Interact*, 2007, **20**, 1421–1430.
147 K. Thedieck, T. Hain, W. Mohamed, B. J. Tindall, M. Nimtz, T. Chakraborty, J. Wehland and L. Jänsch, *Mol. Microbiol.*, 2006, **62**, 1325–1339.
148 R. Kumariya, S. K. Sood, Y. S. Rajput, N. Saini and A. K. Garsa, *Biochim. Biophys. Acta, Biomembr.*, 2015, **1848**, 1367–1375.
149 S. R. Dennison, F. Harris, M. Mura and D. A. Phoenix, *Curr. Protein Pept. Sci.*, 2018, **19**, 823–838.
150 E. Cox, A. Michalak, S. Pagentine, P. Seaton and A. Pokorny, *Biochim. Biophys. Acta*, 2014, **1838**, 2198–2204.
151 L. Assoni, B. Milani, M. R. Carvalho, L. N. Nepomuceno, N. T. Waz, M. E. S. Guerra, T. R. Converso and M. Darrieux, *Front. Microbiol.*, 2020, **11**, 593215.
152 N. N. Mishra, S. J. Yang, A. Sawa, A. Rubio, C. C. Nast, M. R. Yeaman and A. S. Bayer, *Antimicrob. Agents Chemother.*, 2009, **53**, 2312–2318.
153 H. S. Joo and M. Otto, *Biochim. Biophys. Acta*, 2015, **1848**, 3055–3061.
154 D. Song, H. Jiao and Z. Liu, *Nat. Commun.*, 2021, **12**, 2927.
155 K. L. Nawrocki, E. K. Crispell and S. M. McBride, *Antibiotics*, 2014, **3**, 461–492.
156 T. J. Silhavy, D. Kahne and S. Walker, *Cold Spring Harbor Perspect. Biol.*, 2010, **2**, a000414.
157 P. Nikolic and P. Mudgil, *Microorganisms*, 2023, **11**, 259.
158 N. Malanovic and K. Lohner, *Pharmaceuticals*, 2016, **9**, DOI: **10.3390/ph9030059**.
159 N. Preußke, F. D. Sönnichsen and M. Leippe, *Biosci. Rep.*, 2023, **43**, DOI: **10.1042/BSR20230474**.
160 R. Vaiwala, P. Sharma and K. Ganapathy Ayappa, *Biointerphases*, 2022, **17**, 061008.
161 A. Guyet, A. Alofi and R. A. Daniel, *mBio*, 2023, **14**, e0266722.
162 N. Dong, X. Yang, E. W. Chan, R. Zhang and S. Chen, *EBioMedicine*, 2022, **79**, 103998.
163 A. Hadjicharalambous, N. Bournakas, H. Newman, M. J. Skynner and P. Beswick, *Antibiotics*, 2022, **11**, 1636.
164 D. A. Phoenix, F. Harris and S. R. Dennison, *Curr. Protein Pept. Sci.*, 2021, **22**, 775–799.
165 E. Malik, S. R. Dennison, F. Harris and D. A. Phoenix, *Pharmaceuticals*, 2016, **9**, 31–39.
166 D. I. Andersson, D. Hughes and J. Z. Kubicek-Sutherland, *Drug Resist Updat*, 2016, **26**, 43–57.
167 J. Andrä, T. Goldmann, C. M. Ernst, A. Peschel and T. Gutsmann, *J. Biol. Chem.*, 2011, **286**, 18692–18700.
168 G. S. Dijksteel, M. M. W. Ulrich, E. Middelkoop and B. K. H. L. Boekema, *Front. Microbiol.*, 2021, **12**, 37.
169 M. Dostert, C. R. Belanger and R. E. W. Hancock, *J. Innate Immun.*, 2018, **11**, 193–204.
170 M. Kazemzadeh-Narbat, H. Cheng, R. Chabok, M. M. Alvarez, C. de la Fuente-Nunez, K. S. Phillips and A. Khademhosseini, *Crit. Rev. Biotechnol.*, 2021, **41**, 94–120.
171 Y. Zhu, W. Hao, X. Wang, J. Ouyang, X. Deng, H. Yu and Y. Wang, *Med. Res. Rev.*, 2022, **42**, 1377–1422.
172 F. Bugli, C. Martini, M. Di Vito, M. Cacaci, D. Catalucci, A. Gori, M. Iafisco, M. Sanguinetti and A. Vitali, *Microbiol. Res.*, 2022, **263**, 127152.